Cytokine 70 (2014) 194–197

Contents lists available at ScienceDirect

Cytokine

journal homepage: www.journals.elsevier.com/cytokine

Short Communication

High serum osteopontin levels in pediatric patients with high risk Langerhans cell histiocytosis

Yukiko Oh [a], Akira Morimoto [a,*], Yoko Shioda [b], Toshihiko Imamura [c], Kazuko Kudo [d], Shinsaku Imashuku [e], for the Japan LCH Study Group

[a] Department of Pediatrics, Jichi Medical University School of Medicine, Shimotsuke, Japan
[b] Division of Pediatric Oncology, National Center for Child Health and Development, Tokyo, Japan
[c] Department of Pediatrics, Kyoto Prefectural University of Medicine, Kyoto, Japan
[d] Division of Hematology and Oncology, Shizuoka Children's Hospital, Shizuoka, Japan
[e] The Japan LCH Study Group, Kyoto, Japan

ARTICLE INFO

Article history:
Received 18 January 2014
Received in revised form 18 June 2014
Accepted 7 July 2014
Available online 30 July 2014

Keywords:
Langerhans cell histiocytosis
Osteopontin
Serum
Infant
Multisystem disease

ABSTRACT

Osteopontin (OPN) acts as an osteoclast activator, a proinflammatory cytokine, and a chemokine attracting histiocytes/monocytes and is abundantly expressed in Langerhans cell histiocytosis (LCH). We investigated whether serum OPN levels are related to disease types in LCH. Fifty-eight newly diagnosed LCH patients were studied; eight with risk organ (liver, spleen and/or hematopoietic) involvements positive multisystem (MS+) disease, 27 with risk organ involvement negative multisystem (MS−) disease and 23 with single system (SS) disease. Pediatric patients with non-inflammatory disease ($n = 27$) were used as controls. All of patients with MS+ disease were younger than 3 years. Serum OPN levels and 44 kinds of humoral factors were measured by ELISA and Bio-Plex suspension array system, respectively. In the patients younger than 3 years, the median serum OPN level (interquartile range) was 240.3 ng/ml (137.6–456.0) in MS+ ($n = 8$); 92.7 ng/ml (62.0–213.8) in MS− ($n = 14$) and 72.5 ng/ml (55.6–94.0) in SS ($n = 9$) and 74.4 ng/ml (42.2–100.0) in control ($n = 12$). The OPN values were significantly higher in the MS+ group than the MS−, SS and control groups ($p = 0.044$, $p = 0.001$ and $p = 0.002$, respectively), but not different between the MS−, SS and control groups. In the patients older than 3 years, the median level of serum OPN (IQR) was 56.2 ng/ml (22.9–77.5) in MS− ($n = 13$), 58.9 ng/ml (31.0–78.7) in SS ($n = 14$) and 41.9 (28.9–54.1) in control ($n = 15$). These values did not differ significantly between each group. The serum OPN levels were positively correlated with the serum IL-6, CCL2, IL-18, IL-8 and IL-2 receptor concentration. OPN may be involved in risk organ dissemination and poor prognosis of LCH through the function as inflammatory cytokine/chemokine.

1. Introduction

Langerhans cell histiocytosis (LCH) is a proliferative disease of immature dendritic cell (iDC), and has characteristics of a clonal and an inflammatory disease. Two disease types of LCH are known; multisystem disease (MS) and single system disease (SS). Infants with risk organ (liver, spleen and/or hematopoietic system) involvement positive-MS disease have a dismal prognosis, while children with SS disease have an excellent prognosis [1]. Many inflammatory cytokines and chemokines are involved in the pathogenesis of LCH [2] and recently Allen et al. reported that the pleiotropic cytokine osteopontin (OPN) is abundantly expressed by the abnormal LCH cells [3]. Furthermore, Prasse et al. found that OPN expression is upregulated in bronchoalveolar lavage cells in patients with pulmonary LCH and that overexpression of OPN in rat lungs induces lesions similar to pulmonary LCH [4]. OPN is expressed in various human cells and has a variety of functions that include promoting the generation of T helper (Th)1 and Th17 cells [5], recruiting histiocytes/monocytes [6,7] and activating osteoclasts (OCs) [8].

Abbreviations: OPN, osteopontin; LCH, Langerhans cell histiocytosis; MS, multisystem; SS, single system; iDC, immature dendritic cell; Th, T helper; OCs, osteoclasts; JLSG, the Japan LCH Study Group; MS+, multisystem disease with liver, spleen and/or hematopoietic system involvements; MS−, multisystem disease without liver, spleen or hematopoietic system involvements; IL, interleukin; IL-2R, IL-2 receptor α; IFN, interferon; TNF, tumor necrosis factor; CCL, CC chemokine ligand; CXCL, CXC chemokine ligand; IQR, interquartile range; MGCs, multinucleated giant cells.

* Corresponding author. Address: Department of Pediatrics, Jichi Medical University School of Medicine, 3311-1, Yakushi-ji, Shimotsuke, Tochigi 329-0498, Japan. Tel.: +81 285 58 7366; fax: +81 285 44 6123.
E-mail address: akira@jichi.ac.jp (A. Morimoto).

http://dx.doi.org/10.1016/j.cyto.2014.07.002
1043-4666/

Taken together, these findings imply that OPN must have a role in the pathogenesis as well as disease progression of LCH. In spite of data on OPN in *in vitro* system of LCH studies, clinical OPN data are still limited in patients with LCH [3]. In this study, we therefore investigated whether serum OPN levels are related to disease types, i.e. MS vs SS in patients with LCH.

2. Material and methods

2.1. Patients and sample collection

Blood samples and clinical information were obtained with informed consent from 58 newly diagnosed pediatric LCH patients through the Japan LCH Study Group (JLSG) registry, and from 27 pediatric patients with non-inflammatory diseases in stable state including inherited coagulopathy, thrombophilia and anemia, and resected benign tumor, as controls. The median age of LCH patients were 2.8 years (range: 0.4–12.0). A diagnosis of LCH was confirmed by immunohistochemical staining for CD1a antigen in biopsies of the affected organs. The patients consisted of two groups as follows: those with MS disease and those with SS disease. We defined MS as lesions in several organs, SS as lesions in only one organ. Of the 58 LCH patients, 35 were assigned to the MS group, 23 to the SS group. We divided MS patients into patients with liver, spleen and/or hematopoietic involvements (MS+) and patients without these lesions (MS−). Of the 35 MS patients, 8 were assigned to MS+ group, and all of these patients were younger than 3 years. All but three patients with SS disease had bone lesion(s). This study was approved by the ethics committee of the Jichi Medical University School of Medicine.

2.2. Measurement of osteopontin and other humoral factors in serum

Serum samples were stored at −80 °C prior to assay and not subjected to freeze–thaw cycles. Serum OPN levels were measured using the human OPN Quantikine ELISA Kit (R&D Systems, Minneapolis, USA). Forty-four kinds of serum humoral factors, including interleukin (IL)-1β, IL-1 receptor antagonist, IL-2, IL-2 receptor α (IL-2R), IL-3, IL-4, IL-5, IL-6, IL-7, IL-8, IL-9, IL-10, IL-12p40, IL-12p70, IL-13, IL-15, IL-16, IL-17, IL-18, interferon (IFN)-α2, IFN-γ, tumor necrosis factor (TNF)-α, TNF-β, macrophage inhibitory factor, granulocyte-colony stimulating factor, macrophage-colony stimulating factor, granulocyte–macrophage colony-stimulating factor, stem cell factor, leukemia inhibitory factor, fibroblast growth factor basic, hepatocyte growth factor, nerve growth factor-β, vascular endothelial cell growth factor, tumor necrosis factor-related apoptosis inducing ligand, CC chemokine ligand (CCL)2, CCL3, CCL4, CCL7, CCL11, CCL27, CXC chemokine ligand (CXCL) 1, CXCL9, CXCL10 and CXCL12, were measured using Bio-Plex suspension array system (BIO-RAD Laboratories, Hercules, USA).

2.3. Statistical analysis

A Student's *t*-test was used for analyzing normally distributed data (age), and the Mann–Whitney U test for non-normally distributed data (serum OPN level). $P < 0.05$ was regarded as significant. All the data were analyzed using Statcel3 software (OMS Publishing Inc., Saitama, Japan).

3. Results and discussion

The scattergram of serum OPN level and age of the MS, SS and control groups is shown in Fig. 1A. Patients with remarkably high levels of serum OPN were infants younger than 3-years-old with MS disease. Therefore, we analyzed serum OPN levels separately in the two groups: younger or older than 3 years. The younger group consisted of 8 MS+, 14 MS−, 9 SS and 12 controls, while the older group consisted of 13 MS−, 14 SS and 15 controls. In the younger group, the median level of serum OPN was 240.3 ng/ml (interquartile range (IQR), 137.6–456.0) in MS+, 92.7 ng/ml (IQR, 62.0–213.8) in MS−, 72.5 ng/ml (IQR, 55.6–94.0) in SS ($n = 9$) and 74.4 ng/ml (IQR, 42.2–100.0) in control ($n = 12$) groups, respectively. The serum OPN level in MS+ patients was significantly higher than that in MS−, SS and control ($p = 0.044$, $p = 0.001$ and $p = 0.002$, respectively) (Fig. 1B), but did not differ significantly between MS−, SS and control (MS− vs SS: $p = 0.284$, MS− vs control: $p = 0.181$ and SS vs control: $p = 0.239$). In the older group, the median level of serum OPN was 56.2 ng/ml (IQR, 22.9–77.5) in MS−, 58.9 ng/ml (IQR, 31.0–78.7) in SS and 41.9 ng/ml (IQR, 28.9–54.1) in control patents, respectively. The serum OPN level did not differ significantly between these patents (Fig. 1C).

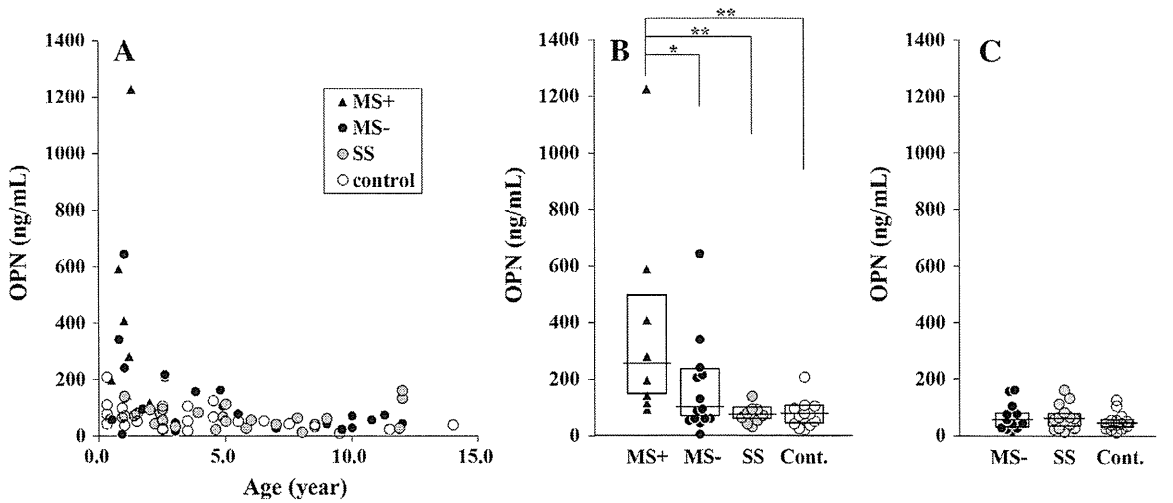

Fig. 1. Serum OPN levels are high in the MS+ patients. (A) Scattergram of serum OPN level and age in all patients. Black triangles, MS+ patients ($n = 8$); black circles, MS− patients ($n = 27$); gray circles, SS patients ($n = 23$); open circles, control ($n = 27$). (B) Comparison of serum OPN levels in patients younger than 3 years. MS + patients ($n = 8$), MS− patients ($n = 14$), SS patients ($n = 9$), control ($n = 12$). $^{*}p < 0.05$; $^{**}p < 0.001$. Bars in boxes indicate the median value, boxes indicate the interquartile range. (C) Comparison of serum OPN levels in patients older than 3 years. MS− patients ($n = 13$), SS patients ($n = 14$), control ($n = 15$). Bars in boxes indicate the median value, boxes indicate the interquartile range.

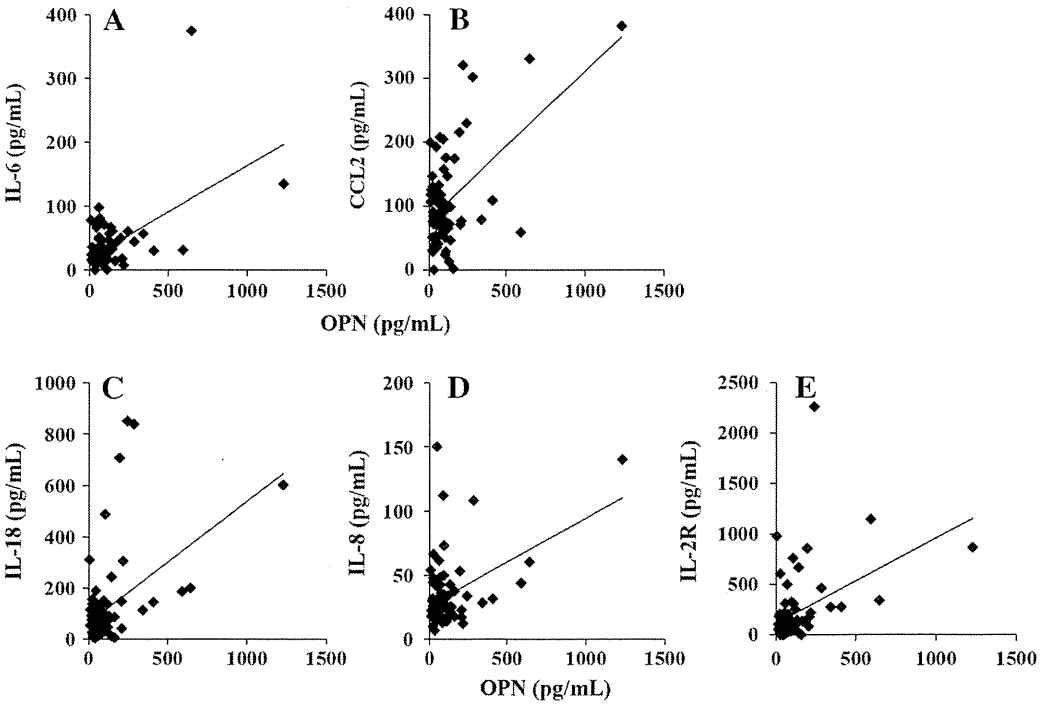

Fig. 2. Serum OPN levels are positively correlated with serum levels of inflammatory cytokine/chemokine of and an immune activation marker. (A) IL-6: $r = 0.545$, $n = 78$, $p < 0.001$. (B) CCL2: $r = 0.543$, $n = 78$, $p < 0.001$. (C) IL-18: $r = 0.477$, $n = 79$, $p < 0.001$. (D) IL-18: $r = 0.447$, $n = 78$, $p < 0.001$. (E) IL-2R: $r = 0.429$, $n = 79$, $p < 0.001$.

Thus, it was concluded that significantly high serum OPN levels were not due to younger age alone but related to the risk organ involvement.

The serum OPN level was positively correlated with the serum IL-6, CCL2, IL-18, IL-8 and IL-2 receptor concentrations (correlation coefficient of 0.545, 0.543, 0.477, 0.447 and 0.429, respectively) (Fig. 2).

Many inflammatory cytokines and chemokines are involved in the pathogenesis of LCH. Inflammatory cytokines are expressed abundantly in LCH lesions [9] and lesional LCH cells produce inflammatory chemokines [10], suggesting that they play an important role in development of LCH. Costa et al. report that OC-like multinucleated giant cells (MGCs) are present in LCH lesions including non-bone lesions [11]. It is hypothesized that these MGCs are formed by the fusion of LCH cells [12]. A possible role for OPN in the pathogenesis of LCH was recently suggested [3,4]. Two reports described high levels of OPN mRNA expression in LCH cells [3,13]. In terms of the correlation with disease types, OPN mRNA expression was found to be up-regulated in LCH cells either from MS or from SS LCH patients; however, the comparative association of the OPN expression levels with disease types was not examined in these reports.

OPN involves (1) promoting the generation of inflammatory cytokine [5], (2) recruiting histiocytes/monocytes [6,7] and (3) activating OCs [8]. In addition we reported that OPN plays a crucial role in the fusion of iDC to form OC-like MGCs [14]. Our study revealed that serum OPN levels are higher in the infants with MS+ LCH compare to the infants with other type of LCH, and that the serum OPN levels are positively correlated with serum levels of inflammatory cytokine/chemokine of and an immune activation marker, including IL-6, CCL2, IL-18, IL-8 and IL-2R. These suggest that high serum OPN values may reflect risk organ dissemination and poor prognosis of LCH through the function as inflammatory cytokine/chemokine rather than OC activator, particularly in infants.

We are aware that this study has limitations. Firstly, we attempted to measure full-length OPN in serum where there is a risk of cleavage of full-length OPN by thrombin during a coagulation process. Thus, full-length OPN is recommended to be measured preferably in plasma. Accordingly, although the data are preliminary, we believe that this study clearly showed the sufficient and meaningful role of OPN in LCH. Secondly, because of small sample size, it was not possible to evaluate the impact of serum OPN levels on the prognosis of patients with MS type of LCH. *In vitro* system, thrombin-cleaved OPN has a higher inflammatory potential than full-length OPN [5]. The correlation between plasma full-length/thrombin-cleaved OPN levels and treatment response or reactivation of LCH as well as outcome of the disease remains to be clarified in future.

Acknowledgments

The authors thank the physicians participating in the JLSG registration program, and Yasuko Hashimoto for her contribution at the JLSG registration center. This study was supported by a grant for Research on Measures for Intractable Diseases from the Ministry of Health, Labor and Welfare, Japan (Grant Reference Number: H24-General-076) and Grant-in-Aid for Scientific Research (KAKENHI) from the Ministry of Education, Culture, Sports, Science and Technology, Japan (Grant Reference Number: 22591167 and 25461606).

References

[1] Morimoto A, Oh Y, Shioda Y, et al. Recent advances in Langerhans cell histiocytosis. Pediatr Int 2014 May 19. http://dx.doi.org/10.1111/ped.123800. [Epub ahead of print].
[2] Garabedian L, Struyf S, Opdenakker G, et al. Langerhans cell histiocytosis: a cytokine/chemokine-mediated disorder? Eur Cytokine Netw 2011;22:148–53.
[3] Allen CE, Li L, Peters TL, et al. Cell-specific gene expression in Langerhans cell histiocytosis lesions reveals a distinct profile compared with epidermal Langerhans cells. J Immunol 2010;184:4557–67.
[4] Prasse A, Stahl M, Schulz G, et al. Essential role of osteopontin in smoking-related interstitial lung diseases. Am J Pathol 2009;174:1683–91.
[5] Uede T. Osteopontin, intrinsic tissue regulator of intractable inflammatory diseases. Pathol Int 2011;61:265–80.

[6] Lund SA, Wilson CL, Raines EW, et al. Osteopontin mediates macrophage chemotaxis via α4 and α9 integrins and survival via the α4 integrin. J Cell Biochem 2013;114:1194–202.
[7] Zheng W, Li R, Pan H, et al. Role of osteopontin in induction of monocyte chemoattractant protein 1 and macrophage inflammatory protein 1beta through the NF-kappa B and MAPK pathways in rheumatoid arthritis. Arthritis Rheum 2009;60:1957–65.
[8] Nakamura I, Duong le T, Rodan SB, et al. Involvement of alpha(v)beta3 integrins in osteoclast function. J Bone Miner Metab 2007;25:337–44.
[9] Egeler RM, Favara BE, van Meurs M, et al. Differential In situ cytokine profiles of Langerhans-like cells and T cells in Langerhans cellhistiocytosis: abundant expression of cytokines relevant to disease and treatment. Blood 1999;94:4195–201.
[10] Annels NE, da Costa CE, Prins FA, et al. Aberrant chemokine receptor expression and chemokine production by Langerhans cells underlies the pathogenesis of Langerhans cell histiocytosis. J Exp Med 2003;197:1385–90.
[11] da Costa CE, Annels NE, Faaij CM, et al. Presence of osteoclast-like multinucleated giant cells in the bone and nonostotic lesions of Langerhans cell histiocytosis. J Exp Med 2005;201:687–93.
[12] Coury F, Annels N, Rivollier A, et al. Langerhans cell histiocytosis reveals a new IL-17A–dependent pathway of dendritic cell fusion. Nat Med 2008;14:81–7.
[13] Hutter C, Kauer M, Simonitsch-Klupp I, et al. Notch is active in Langerhans cell histiocytosis and confers pathognomonic features on dendritic cells. Blood 2012;120:5199–208.
[14] Oh Y, Oh I, Morimoto J, et al. Osteopontin has a crucial role in osteoclast-like multinucleated giant cell formation. J Cell Biochem 2014;115:585–95.

Peripheral blood lymphocyte telomere length as a predictor of response to immunosuppressive therapy in childhood aplastic anemia

Hirotoshi Sakaguchi,[1,2]* Nobuhiro Nishio,[1]* Asahito Hama,[1] Nozomu Kawashima,[1] Xinan Wang,[1] Atsushi Narita,[1] Sayoko Doisaki,[1] Yinyan Xu,[1] Hideki Muramatsu,[1] Nao Yoshida,[2] Yoshiyuki Takahashi,[1] Kazuko Kudo,[3] Hiroshi Moritake,[4] Kazuhiro Nakamura,[5] Ryoji Kobayashi,[6] Etsuro Ito,[7] Hiromasa Yabe,[8] Shouichi Ohga,[9] Akira Ohara,[10] and Seiji Kojima;[1] on behalf of the Japan Childhood Aplastic Anemia Study Group

[1]Department of Pediatrics, Nagoya University Graduate School of Medicine; [2]Division of Hematology and Oncology, Children's Medical Center, Japanese Red Cross Nagoya 1st Hospital; [3]Division of Hematology and Oncology, Shizuoka Children's Hospital; [4]Division of Pediatrics, Department of Reproductive and Developmental Medicine, Faculty of Medicine, University of Miyazaki; [5]Department of Pediatrics, Hiroshima University Graduate School of Biomedical and Health Sciences; [6]Department of Pediatrics, Sapporo Hokuyu Hospital; [7]Department of Pediatrics, Hirosaki University Graduate School of Medicine; [8]Department of Cell Transplantation and Regenerative Medicine, Tokai University School of Medicine, Isehara; [9]Department of Perinatal and Pediatric Medicine, Graduate School of Medical Sciences, Kyushu University, Fukuoka; and [10]Department of Pediatrics, Toho University School of Medicine, Tokyo, Japan

HS and NN contributed equally to this work.

ABSTRACT

Predicting the response to immunosuppressive therapy could provide useful information to help the clinician define treatment strategies for patients with aplastic anemia. In our current study, we evaluated the relationship between telomere length of lymphocytes at diagnosis and the response to immunosuppressive therapy in 64 children with aplastic anemia, using flow fluorescence *in situ* hybridization. Median age of patients was ten years (range 1.5-16.2 years). Severity of the disease was classified as very severe in 23, severe in 21, and moderate in 20 patients. All patients were enrolled in multicenter studies using antithymocyte globulin and cyclosporine. The response rate to immunosuppressive therapy at six months was 52% (33 of 64). The probability of 5-year failure-free survival and overall survival were 56% (95% confidence interval (CI): 41-69%) and 97% (95%CI: 87-99%), respectively. Median telomere length in responders was -0.4 standard deviation (SD) (-2.7 to +3.0 SD) and -1.5 SD (-4.0 to +1.6 (SD)) in non-responders (P<0.001). Multivariate analysis showed that telomere length shorter than -1.0 SD (hazard ratio (HR): 22.0; 95%CI: 4.19-115; P<0.001), platelet count at diagnosis less than 25x10^9/L (HR: 13.9; 95%CI: 2.00-96.1; P=0.008), and interval from diagnosis to immunosuppressive therapy longer than 25 days (HR: 4.81; 95%CI: 1.15-20.1; P=0.031) were the significant variables for poor response to immunosuppressive therapy. Conversely to what has been found in adult patients, measurement of the telomere length of lymphocytes at diagnosis is a promising assay in predicting the response to immunosuppressive therapy in children with aplastic anemia.

Introduction

Aplastic anemia (AA) is defined as bone marrow aplasia and peripheral blood pancytopenia; disease pathogenesis is thought to involve immune-mediated processes. The first choice of treatment for severe AA in children is hematopoietic stem cell transplantation from a human leukocyte antigen (HLA)-matched sibling donor.[1,2] However, 60-70% of children with severe AA have no matched sibling donor and receive immunosuppressive therapy (IST), consisting of antithymocyte globulin (ATG) and cyclosporine (CyA). According to previous studies in children, the response rate to IST at six months was 60-70%, with the probability of survival at five years being over 90%. On the other hand, relapses occur in 10-30% of patients who responded to IST and, overall, clonal evolution develops in 10-15% patients.[3-5] In adults, several pre-treatment biomarkers have been proposed as promising tests for predicting favorable response to IST, including the presence of either human leukocyte antigen (HLA)-DR15 or a minor population of paroxysmal nocturnal hemoglobinuria (PNH)-type cells.[6-9] However, we previously reported that neither test was useful to predict response to IST and that lower white blood cell count and shorter interval from diagnosis to IST were significant predictive markers of better response,[10] on the other hand, a National Institutes of Health (NIH) study showed that higher base-line absolute reticulocyte and lymphocyte counts were highly predictive of response to IST in adult patients.[11] These results suggest a difference in etiology of AA between adults and children.[10]

Dyskeratosis congenita (DC) is a rare inherited disease characterized by the classical mucocutaneous triad of abnormal skin pigmentation, nail dystrophy, and mucosal leukoplakia.[12] Patients with DC are unable to maintain the telomere complex that are protein-DNA structures at the end of eukaryotic chromosomes that prevent degradation and aberrant recombination of the chromosome ends,[13,14] and consequently have very short telomeres.[15] Shortened telomeres can cause a wide variety of clinical features consisting not only of

 doi:10.3324/haematol.2013.091165
The online version of this article has a Supplementary Appendix.
Manuscript received on May 12, 2013. Manuscript accepted on April 28, 2014.
Correspondence: kojimas@med.nagoya-u.ac.jp

mucocutaneous abnormalities, but also other symptoms, including bone marrow failure, pulmonary fibrosis, hepatic fibrosis, and predisposition to malignancy.[16] Several recent studies revealed cryptic forms of DC among patients with seemingly acquired AA who did not have apparent physical abnormalities.[17,18] Failure of AA patients to respond to IST may be explained by the presence of cryptic inherited bone marrow failure syndromes (IBMFSs).

Several investigators have demonstrated that telomere lengths of leukocytes in patients with AA vary widely, with an increased proportion of the patients having shorter telomeres than healthy individuals.[19,20] It is known that not only patients with typical DC, but also those with cryptic DC have very short telomeres.[21] Moreover, the telomere length in leukocytes is decreased in subsets of patients with other IBMFSs including Fanconi anemia,[22] Diamond-Blackfan anemia,[23] and Schwachman-Diamond syndrome.[24] Therefore, measuring telomere length of patients with AA at diagnosis may be useful in detecting patients with cryptic type of IBMFSs.

Recently, Scheinberg *et al.* reported that the telomere length of peripheral blood leukocytes was associated with risk of hematologic relapse, clonal evolution to myelodysplastic syndrome, and overall survival (OS), but not related to hematologic response to IST in patients with severe AA.[25] Because there was no study to validate their observation, we evaluated the relationship between telomere length in hematopoietic cells before IST and the response to IST in children with AA.

Methods

Patients

Peripheral blood samples at diagnosis and clinical records were obtained from 64 children who fulfilled entry criteria and enrolled in two prospective studies conducted by the Japan Childhood Aplastic Anemia Study Group.[26,27] Patients with acquired AA were eligible if selection criteria were satisfied (see *Online Supplementary Appendix* for details). Thirty-eight patients received horse ATG (Lymphoglobulin; Genzyme, Cambridge, MA, USA) at 15 mg/kg/day for five days and 26 received rabbit ATG (Thymoglobulin, Genzyme, Cambridge, MA, USA) at 3.75 mg/kg/day for five days. CyA (6 mg/kg/day, orally) was started on Day 1 and continued to at least Day 180. The dose was adjusted to achieve a whole blood trough level of 100-200 ng/mL. Standard supportive care was supplied in each institute. Response to IST was evaluated according to previously described criteria.[3] We defined patients with complete response or partial response at six months after IST as responders, and the other patients as non-responders. Relapse was defined by conversion to no response from a partial or complete response and/or the requirement for blood transfusions.

All samples and clinical records were collected after written informed consent had been obtained according to protocols approved by the Ethics Review Committee, Nagoya University Graduate School of Medicine (Research n. 732).

Measurements of telomere length and population of PNH clones

The average relative telomere length (RTL) of peripheral lymphocytes was measured by flow fluorescence *in situ* hybridization (flow-FISH), using a Telomere PNA kit (Dako Cytomation, Glostrup, Denmark).[28] Lymphocytes were derived from fresh peripheral blood in 38 cases and from frozen stored peripheral blood in 26 cases. We used delta RTL to compare patients' telomere length with that of age-matched healthy controls. Details of methods for measuring telomere length and definition of delta RTL are described in the *Online Supplementary Methods*. A minor population of paroxysmal nocturnal hemoglobinuria (PNH)-type granulocytes and red blood cells were also evaluated by flow cytometry according to a previously described method.[10]

Statistical analysis

We analyzed predictive variables associated with response to IST, failure-free survival (FFS; in which relapse, clonal evolution, second IST, HSCT, and death were censored), transplantation-free survival (TFS; in which HSCT and death were censored), and OS. Pre-treatment variables included patient's sex, age, etiology, disease severity, interval from diagnosis to IST, leukocyte count, lymphocyte count, neutrophil count, hemoglobin (Hb) level, platelet count, reticulocyte count, presence of HLA-DR15, presence of minor PNH clone, and delta RTL. Differences in these variables between responders and non-responders were assessed using the Mann-Whitney U-test and Fisher's exact probability test. Predictive factors with $P<0.10$ in the univariate analyses were set in the multivariate analysis (logistic regression modeling). $P<0.05$ was considered statistically significant. Measures of association were expressed as hazard ratios (HR) with 95% confidence intervals (CI). All tests were two-tailed with a type I error of less than 0.05 considered as statistically significant. All analyses were performed using STATA12.0 software (STATA, College Station, TX, USA).

Results

Pre-treatment patients' characteristics and clinical outcomes

A total of 64 patients with AA were included in this study. Patients' characteristics are shown in Table 1. The median age at IST was 10.0 years (range 1.5-16.2 years). Disease severity was assessed as very severe in 23 patients, severe in 21 patients, and moderate in 20 patients. Causes of AA were idiopathic in 60 patients and hepatitis in 4 patients. Median follow-up time from the time of IST was 35 months (range 6-132 months).

Overall, 33 of 64 patients (52%) responded to IST at six months after administration of ATG. Of the 33 responders, 4 children relapsed at 6, 34, 66, and 91 months after IST, respectively. The probability of 5-year cumulative incidence of relapse was 8% (95%CI: 2-28%). Nineteen transplantations were carried out for non-responders or patients with relapse. Of 64 children with AA, only one patient developed clonal evolution at 23 months after IST. During the observation period, 2 patients died; both of them had shown no response to IST, one suffered from lethal cerebral hemorrhage at six months, and the other underwent bone marrow transplantation from an HLA-matched unrelated donor at 12 months after IST and died of transplantation-related hepatic failure. The probability of 5-year FFS, TFS, and OS were 56% (95%CI: 41-69%), 63% (95%CI: 48-75%), and 97% (95%CI: 87-99%), respectively.

Telomere length of children with AA

Comparing SD calculated in 71 healthy individuals, median telomere length was -0.9SD (range -4.0 to +3.0SD) in all patients (n=64), -0.4SD (range -2.7 to +3.0SD) in

Table 1. Patients' characteristics.

Variables		Total	Responder	Non-responder	P
N		64	33	31	
Sex	M/F	38 / 26	22 / 11	16 / 15	NS
Age at diagnosis (range)	median	10.0 (1.5-16.2)	10.0 (1.5-16.2)	9.7 (2.6-15.1)	NS
Severity	VSAA/ SAA/MAA	23/21/20	12/10/11	11/11/9	NS
Etiology	Idiopathic/hepatitis	60/4	31/2	29/2	NS
ATG	Horse/rabbit	38/26	23/10	15/16	0.08
Interval from diagnosis to IST	median (range)	22 (1-341)	18 (1-85)	28 (4-341)	0.02
WBC at diagnosis ($x10^6$/L)	median (range)	2300 (20-8700)	2300 (20-8700)	2400 (300-5000)	NS
NEU at diagnosis ($x10^6$/L)	median (range)	300 (0-3130)	380 (0-3130)	260 (0-1140)	NS
LYM at diagnosis ($x10^6$/L)	median (range)	1900 (20-5600)	1800 (20-5600)	2000 (200-4300)	NS
Hb at diagnosis (g/dL)	median (range)	7.3 (2.7-11.4)	7.2 (2.8-11.0)	7.4 (2.7-11.4)	NS
PLT at diagnosis ($x10^9$/L)	median (range)	1.6 (0.3-5.4)	2.1 (0.4-5.2)	1.6 (0.3-5.4)	0.04
RET at diagnosis ($x10^9$/L)	median (range)	27 (0-96)	27 (3-96)	27 (0-75)	NS
PNH clone	Positive/negative	11 / 53	7 / 26	4 / 27	NS
HLA-DR15	Positive/negative	20 / 44	13 / 20	7 / 24	NS
delta RTL (SD)	median (range)	-0.9 (-4.0 - +3.0)	-0.4 (-2.8 - +3.0)	-1.5 (-4.0 - +1.6)	<0.001

ATG: antithymocyte globulin; F: female; Hb: hemoglobin; HLA: human leukocyte antigen; IST: immune suppressive therapy; LYM: lymphocyte count; M: male; MAA: moderate aplastic anemia; NEU: neutrophil count; NS: not significant; PLT: platelet count; PNH: paroxysmal nocturnal hemoglobinuria; RET: reticulocyte count; RTL: relative telomere length; SAA: severe aplastic anemia; SD: standard deviation; VSAA: very severe aplastic anemia; WBC: white blood cell count.

Table 2. Multivariate analyses for poor response to IST, failure-free survival, and transplantation-free survival.

	HR	95% CI	P
Multivariate analysis for response to IST			
Interval from diagnosis to IST >25 days	4.81	1.15-20.1	0.031
IST with rabbit ATG	0.79	0.16-3.96	0.77
PLT <25x10^9/L	13.9	2.00-96.1	0.008
RTL <-1SD	22	4.19-115	<0.001
Multivariate analysis for FFS			
IST with rabbit ATG	1.27	0.47-3.48	0.64
LYM >2.0x10^9/L	2.32	1.02-5.24	0.044
PLT <25x10^9/L	4.11	1.17-14.5	0.028
RTL <-1SD	2.01	0.83-4.89	0.12
Multivariate analysis for TFS			
IST with rabbit ATG	1.32	0.45-3.86	0.61
LYM >2.0x10^9/L	3.42	1.32-8.81	0.011
PLT <25x10^9/L	4.64	1.00-21.6	0.051
RTL <-1SD	2.84	1.01-7.97	0.048

ATG: antithymocyte globulin; CI: confidence interval; FFS: failure-free survival; HR: hazard ratio; IST: immunosuppressive therapy; LYM: lymphocyte count; PLT: platelet count; RTL: relative telomere length; SD: standard deviation; TFS: transplantation-free survival; MAA: moderate aplastic anemia; NEU: neutrophil count; NS: not significant; PLT: platelet count; PNH: paroxysmal nocturnal hemoglobinuria; RET: reticulocyte count; RTL: relative telomere length; SAA: severe aplastic anemia; SD: standard deviation; VSAA: very severe aplastic anemia; WBC: white blood cell count.

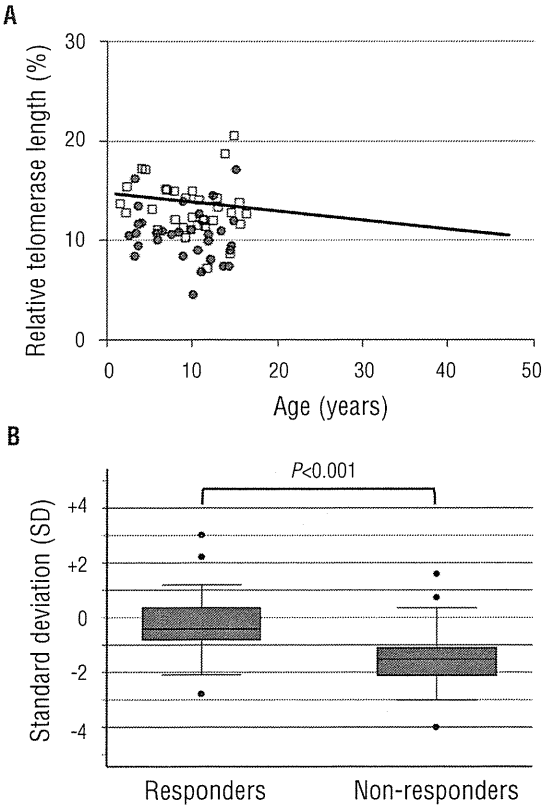

Figure 1. Relative telomere length in responders and non-responders. (A) Scatter plot of relative telomere length (RTL) *versus* age in patients with aplastic anemia (AA). The regression line for healthy individuals is shown as a solid line (Y= -0.0907X + 14.751). Results for AA patients were shown for responders (n=33; open squares) and non-responders (n=31; closed circles). (B) Comparison for telomere length between responders and non-responders. Box plots representing the distribution of telomere length in responders (n=33) and non-responders (n=31). The upper and lower limits of the boxes represent the 75th and 25th percentiles, respectively; the horizontal bar across the box indicates the median and the ends of the vertical lines indicate the minimum and maximum data values. Dots indicate outliers.

responders (n=33), and -1.5SD (range -4.0 to +1.6SD) in non-responders (n=31) (Figure 1A and B). There was a significant difference in telomere length between responders and non-responders (P<0.001). We evaluated the effects of age-adjusted telomere length quartiles on the response rate. There was a significant relationship between hematologic response and telomere length. The response rates at six months were 12.5% in the first (the shortest), 37.5% in the second, 75% in the third, and 81.3% in the fourth (the longest) quartiles of telomere length (Figure 2). The most powerful cut-off point for dividing responders and non-responders by telomere length was -1.0 SD (P=6.9x10^{-6}). There was no statistical tendency between relapse rate / clonal evolution / overall survival and telomere length.

We evaluated the pre-treatment variables for predicting response to IST in 64 children with AA (Table 1). Univariate analysis showed that interval from diagnosis to IST longer than 25 days (P=0.01), platelet count at diagnosis less than 25x10^9/L (P=0.01), and telomere length shorter than -1SD

(P<0.001) were the variables statistically significant for poor response to IST, while there were no significant differences between responders and non-responders in terms of patient age, sex, disease severity, WBC count, neutrophil count, lymphocyte count, reticulocyte count, presence of HLA-DR15, and presence of minor PNH clones. Patients with rabbit ATG showed a tendency of poorer response to IST than patients with horse ATG (P=0.08).

Multivariate analysis confirmed that telomere length shorter than -1.0SD (HR 22.0; 95%CI: 4.19-115; P<0.001), platelet count at diagnosis less than 25x10^9/L (HR 13.9; 95%CI: 2.00-96.1; P=0.008), and interval from diagnosis to IST longer than 25 days (HR 4.81; 95%CI: 1.15-20.1; P=0.031) were the significant predictive variables for poor response to IST (Table 2).

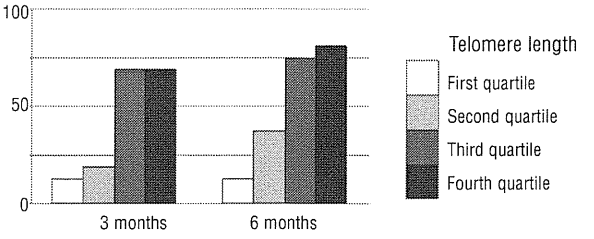

Figure 2. Response rates for immune suppressive therapy at three and six months according to telomere length. A poorer response rate was observed with each quartile as the telomere length shortened from the fourth to the first quartile.

Discussion

Our study demonstrated that the measurement of telomere length of lymphocytes is useful for predicting the response to IST in patients with AA. Recently, the NIH group reported that the telomere length of peripheral blood leukocytes was not related to hematologic response to IST, but was associated with the high risk of hematologic relapse, clonal evolution to myelodysplastic syndrome, and OS.[25] Several reasons may explain the conflicting results of the two studies. To begin with, there are several differences between the current study and the NIH study, including the methods of telomere length measurement and patients' characteristics. In the NIH study, the telomere length of pre-treatment total leukocytes was assessed by quantitative polymerase chain reaction (PCR). We measured the telomere length of lymphocytes using flow-FISH, which enabled us to measure median telomere length in the subpopulations of blood cells. Alter *et al.* compared the diagnostic sensitivity and specificity of short telomeres in different subpopulations of blood cells.[29] Their results indicated that lymphocytes were more suitable for diagnosis of DC than total leukocytes, which were a heterogeneous mixture of cell populations. The proportions of each cell population were different in each patient. The use of total leukocytes is suspected to provide less consistent results than analyses of defined leukocyte subpopulations.

Another difference between the two studies was the distribution of patients' age. Patients in our study were much younger (mean age 10 years) than those in the NIH study (mean age 35 years). Because telomeres shorten with age,[30] the differences in telomere length between patients and healthy individuals may become smaller in adults than in children. Moreover, in the NIH study, the cohort was restricted to patients with severe AA, and patients with moderate AA were not included. In contrast, 20 of 64 AA patients in our study had moderate disease. We could not estimate the frequency of clonal evolution since in our cohort there was only one patient who evolved into myelodysplastic syndrome during the observation period.

The causes of the difference in telomere length between responders and non-responders remain unknown. The short telomere length in non-responders may be ascribed to the presence of cryptic forms of IBMFS in the study cohort. Alter *et al.* reported that nearly all of the patients with both typical and cryptic DC have very short telomeres, as low as the first percentile of normal controls.[25] In our previous study, the RTLs of lymphocytes were below the 5% of normal controls in all of 6 DC patients and 2 AA patients harboring TERT mutation.[31] In the current study, there were 10 AA patients with shorter telomere length than the -2.0 SD of the cohort of healthy controls, but none of them showed clinical features of DC or had any mutation in *DKC1, TERC, TERT, NOP10, TINF2,* and *TCAB1*. It is unlikely that short telomeres in non-responders are to be ascribed to the presence of a cryptic form of DC.

Another possibility is that short telomere length may be a surrogate marker for longer disease duration that damages the hematopoietic stem cells and causes a higher number of compensatory stem cell divisions. We recently reported a significant inverse correlation between response rate to IST and interval between diagnosis and treatment in a large cohort of 312 children with newly diagnosed AA.[32] It is often difficult to determine the exact date of onset of the disease in patients with AA, especially in patients with moderate AA. The shorter telomere length may simply reflect longer duration of the disease in non-responders.

However, our study has several limitations, including a heterogeneous study population, a relatively small number of patients and a short follow-up period. To validate the results, we are conducting a prospective study to determine the optimal use of rabbit ATG for severe AA, in which we evaluate the relationship between telomere length of lymphocytes at diagnosis and the response to IST.

In conclusion, measurement of the telomere length in lymphocytes by flow-FISH is a promising assay, not only for identifying cryptic DC, but also for predicting the response to IST of patients with AA.

Acknowledgments

The authors would like to thank all contributors associated with the Japan Childhood Aplastic Anemia Study Group.

Funding

The authors supported by a grant from the Research Commitee for the dyskeratosis congenita, Ministry of Halth, and Walfare of Japan (H23-Nanchi-Japan-099) and a grant from Sanofi K.K..

Authorship and Disclosures

Information on authorship, contributions, and financial & other disclosures was provided by the authors and is available with the online version of this article at www.haematologica.org

References

1. Kojima S, Horibe K, Inaba J, Yoshimi A, Takahashi Y, Kudo K, et al. Long-term outcome of acquired aplastic anaemia in children: comparison between immunosuppressive therapy and bone marrow transplantation. Br J Haematol. 2000;111(1):321- 8.
2. Young NS. Acquired aplastic anemia. JAMA. 1999;282(3):271-8.
3. Kojima S, Hibi S, Kosaka Y, Yamamoto M, Tsuchida M, Mugishima H, et al. Immunosuppressive therapy using antithymocyte globulin, cyclosporine, and danazol with or without human granulocyte colony-stimulating factor in children with acquired aplastic anemia. Blood. 2000;96(6):2049-54.
4. Fuhrer M, Rampf U, Baumann I, Faldum A, Niemeyer C, Janka-Schaub G, et al. Immunosuppressive therapy for aplastic anemia in children: a more severe disease predicts better survival. Blood. 2005;106 (6):2102-4.
5. Locasciulli A, Oneto R, Bacigalupo A, Socie G, Korthof E, Bekassy A, et al. Outcome of patients with acquired aplastic anemia given first line bone marrow transplantation or immunosuppressive treatment in the last decade: a report from the European Group for Blood and Marrow Transplantation (EBMT). Haematologica. 2007;92(1):11-8.
6. Nakao S, Takamatsu H, Chuhjo T, Ueda M, Shiobara S, Matsuda T, et al. Identification of a specific HLA class II haplotype strongly associated with susceptibility to cyclosporine-dependent aplastic anemia. Blood. 1994;84(12):4257-61.
7. Maciejewski JP, Follmann D, Nakamura R, Saunthararajah Y, Rivera CE, Simonis T, et al. Increased frequency of HLA-DR2 in patients with paroxysmal nocturnal hemoglobinuria and the PNH/aplastic anemia syndrome. Blood. 2001;98(13):3513-9.
8. Oguz FS, Yalman N, Diler AS, Oguz R, Anak S, Dorak MT. HLA-DRB1*15 and pediatric aplastic anemia. Haematologica. 2002;87(7): 772-4.
9. Sugimori C, Chuhjo T, Feng X, Yamazaki H, Takami A, Teramura M, et al. Minor population of CD55-CD59- blood cells predicts response to immunosuppressive therapy and prognosis in patients with aplastic anemia. Blood 2006;107:1308-14.
10. Yoshida N, Yagasaki H, Takahashi Y, Yamamoto T, Liang J, Wang Y, et al. Clinical impact of HLA-DR15, a minor population of paroxysmal nocturnal haemoglobinuria-type cells, and an aplastic anaemia-associated autoantibody in children with acquired aplastic anaemia. Br J Haematol. 2008;142 (3):427-35.
11. Scheinberg P, Wu CO, Nunez O, Young NS. Predicting response to immunosuppressive therapy and survival in severe aplastic anaemia. Br J Haematol. 2009;144(2):206-16.
12. Walne AJ, Dokal I. Advances in the understanding of dyskeratosis congenita. Br J Haematol. 2009;145:164-72.
13. Greider CW, Blackburn EH. Identification of a specific telomere terminal transferase activity in Tetrahymena extracts. Cell. 1985;43(2 Pt 1):405-13.
14. Szostak JW, Blackburn EH. Cloning yeast telomeres on linear plasmid vectors. Cell. 1982;29(1):245-55.
15. Mitchell JR, Wood E, Collins K. A telomerase component is defective in the human disease dyskeratosis congenita. Nature. 1999;402:551-5.
16. Calado RT, Young NS. Telomere diseases. N Engl J Med. 2009;361:2353-65.
17. Yamaguchi H, Calado RT, Ly H, Kajigaya S, Baerlocher GM, Chanock SJ, et al. Mutations in TERT, the gene for telomerase reverse transcriptase, in aplastic anemia. N Engl J Med. 2005;352(14):1413-24.
18. Vulliamy TJ, Marrone A, Knight SW, Walne A, Mason PJ, Dokal I. Mutations in dyskeratosis congenita: their impact on telomere length and the diversity of clinical presentation. Blood. 2006;107:2680-5.
19. Ball SE, Gibson FM, Rizzo S, Tooze JA, Marsh JC, Gordon-Smith EC. Progressive telomere shortening in aplastic anemia. Blood. 1998;91(10):3582-92.
20. Brummendorf TH, Maciejewski JP, Mak J, Young NS, Lansdorp PM. Telomere length in leukocyte subpopulations of patients with aplastic anemia. Blood. 2001;97(4):895-900.
21. Yamaguchi H, Baerlocher GM, Lansdorp PM, Chanock SJ, Nunez O, Sloand E, Young NS. Mutations of the human telomerase RNA gene (TERC) in aplastic anemia and myelodysplastic syndrome. Blood. 2003;102 (3):916-8.
22. Leteurtre F, Li X, Guardiola P, Le Roux G, Sergère JC, Richard P, et al. Accelerated telomere shortening and telomerase activation in Fanconi's anaemia. Br J Haematol. 1999;105(4):883-93.
23. Pavesi E, Avondo F, Aspesi A, Quarello P, Rocci A, Vimercati C, et al. Analysis of telomeres in peripheral blood cells from patients with bone marrow failure. Pediatr Blood Cancer. 2009;53(3):411-6.
24. Thornley I, Dror Y, Sung L, Wynn RF, Freedman MH. Abnormal telomere shortening in leucocytes of children with Shwachman-Diamond syndrome. Br J Haematol. 2002;117(1):189-92.
25. Scheinberg P, Cooper JN, Sloand EM, Wu CO, Calado RT, Young NS. Association of Telomere Length of Peripheral Blood Leukocytes With Hematopoietic Relapse, Malignant Transformation, and Survival in Severe Aplastic Anemia. JAMA. 2010;304 (12):1358-64.
26. Kosaka Y, Yagasaki H, Sano K, Kobayashi R, Ayukawa H, Kaneko T, et al. Prospective multicenter trial comparing repeated immunosuppressive therapy with stem-cell transplantation from an alternative donor as second-line treatment for children with severe and very severe aplastic anemia. Blood. 2008;111:1054-9.
27. Takahashi Y, Muramatsu H, Sakata N, Hyakuna N, Hamamoto K, Kobayashi R, et al. Rabbit antithymocyte globulin and cyclosporine as first-line therapy for children with acquired aplastic anemia. Blood. 2013;121:862-3.
28. Baerlocher GM, Vulto I, de Jong G, Lansdorp PM. Flow cytometry and FISH to measure the average length of telomeres (flow FISH). Nat Protoc. 2006;1(5):2365-76.
29. Alter BP, Baerlocher GM, Savage SA, Chanock SJ, Weksler BB, Willner JP, et al. Very short telomere length by flow fluorescence in situ hybridization identifies patients with dyskeratosis congenita. Blood. 2007;110(5):1439-47.
30. Harley CB, Futcher AB, Greider CW. Telomeres shorten during ageing of human fibroblasts. Nature. 1990;345(6274):458-60.
31. Nishio N, Kojima S. Recent progress in dyskeratosis congenita. Int J Hematol. 2010;92(3):419-24.
32. Yoshida N, Yagasaki H, Hama A, Takahashi Y, Kosaka Y, Kobayashi R, et al. Predicting response to immunosuppressive therapy in childhood aplastic anemia. Haematologica. 2011;96(5):771-4.

Leukemia (2014) **28**, 2344–2354

www.nature.com/leu

ORIGINAL ARTICLE

Impaired hematopoietic differentiation of *RUNX1*-mutated induced pluripotent stem cells derived from FPD/AML patients

M Sakurai[1], H Kunimoto[1], N Watanabe[2], Y Fukuchi[1], S Yuasa[3], S Yamazaki[4], T Nishimura[5], K Sadahira[1], K Fukuda[3], H Okano[6], H Nakauchi[4,5], Y Morita[7], I Matsumura[7], K Kudo[8], E Ito[8], Y Ebihara[9], K Tsuji[9,10], Y Harada[11,12], H Harada[11,12], S Okamoto[1] and H Nakajima[1]

Somatic mutation of *RUNX1* is implicated in various hematological malignancies, including myelodysplastic syndrome and acute myeloid leukemia (AML), and previous studies using mouse models disclosed its critical roles in hematopoiesis. However, the role of *RUNX1* in human hematopoiesis has never been tested in experimental settings. Familial platelet disorder (FPD)/AML is an autosomal dominant disorder caused by germline mutation of *RUNX1*, marked by thrombocytopenia and propensity to acute leukemia. To investigate the physiological function of *RUNX1* in human hematopoiesis and pathophysiology of FPD/AML, we derived induced pluripotent stem cells (iPSCs) from three distinct FPD/AML pedigrees (FPD-iPSCs) and examined their defects in hematopoietic differentiation. By *in vitro* differentiation assays, FPD-iPSCs were clearly defective in the emergence of hematopoietic progenitors and differentiation of megakaryocytes, and overexpression of wild-type (WT)-*RUNX1* reversed most of these phenotypes. We further demonstrated that overexpression of mutant-*RUNX1* in WT-iPSCs did not recapitulate the phenotype of FPD-iPSCs, showing that the mutations were of loss-of-function type. Taken together, this study demonstrated that haploinsufficient *RUNX1* allele imposed cell-intrinsic defects on hematopoietic differentiation in human experimental settings and revealed differential impacts of *RUNX1* dosage on human and murine megakaryopoiesis. FPD-iPSCs will be a useful tool to investigate mutant *RUNX1*-mediated molecular processes in hematopoiesis and leukemogenesis.

Leukemia (2014) **28,** 2344–2354; doi:10.1038/leu.2014.136

INTRODUCTION

RUNX1 is a founding member of Runt-family transcription factors, which was cloned from a break point of t(8;21) chromosomal translocation observed in acute myeloid leukemia (AML). Studies over a decade have revealed critical roles of *RUNX1* in hematopoiesis. During embryonic development, *Runx1* is absolutely essential in the emergence of hematopoietic stem and progenitor cells through hemogenic endothelium. In contrast, conditional disruption of *Runx1* in adult hematopoietic system revealed that it was critical in the differentiation of megakaryocytes (MgKs) and lymphocytes as well as in the homeostasis of hematopoietic stem cells.[1] However, these results were mostly derived from gene-disruption studies in mice, and the role of *RUNX1* in human hematopoiesis has never been tested in experimental settings.

Somatic mutation of *RUNX1* has been implicated in a variety of hematological malignancies, including myelodysplastic syndrome (MDS) and AML. It was found in 15–35% cases of AML M0 subtype,[2] 10–20% of MDS,[3–6] 37% of chronic myelomonocytic leukemia[7] and 14% of MDS/myeloproliferative neoplasm,[8] which makes *RUNX1* as one of the most frequently mutated genes in hematological malignancies.

The mutations are distributed throughout *RUNX1* protein, being roughly classified into two categories, missense mutation in N-terminal Runt-homology domain and frame-shift or non-sense mutations leading to a C-terminal truncation. Runt-homology domain mutation impairs DNA-binding and nuclear localization, while the C-terminal truncation disrupts transcriptional activation or repression activity.[3,9] Biochemical studies have shown that most of the *RUNX1* mutations observed in MDS or AML are loss-of-function mutation or dominant negative to the residual wild-type (WT) allele.[9–12] However, their capacities to suppress transcriptional activity of WT-*RUNX1* vary among mutants by *in vitro* assays.[3] In addition, it is possible that some mutations confer the protein with non-physiological functions acting as gain-of-function mutants. Therefore, precise function of mutant *RUNX1* in MDS or AML remains obscure, and it must be tested in physiological and, ideally, in human settings.

Familial platelet disorder/AML(FPD/AML) is a rare autosomal dominant disorder caused by germline mutation of *RUNX1*, marked by thrombocytopenia and propensity to acute leukemia.[13] Approximately 30 FPD/AML pedigrees have been reported to date, and the affected patients retained *RUNX1* mutation at similar positions as reported in MDS and AML. Most patients present no

[1]Division of Hematology, Department of Internal Medicine, Keio University School of Medicine, Tokyo, Japan; [2]Department of Transfusion Medicine and Cell Therapy, Keio University School of Medicine, Tokyo, Japan; [3]Division of Cardiology, Department of Internal Medicine, Keio University School of Medicine, Tokyo, Japan; [4]Japan Science and Technology Agency, ERATO, Tokyo, Japan; [5]Division of Stem Cell Therapy, Center for Stem Cell Biology and Regenerative Medicine, The Institute of Medical Science, The University of Tokyo, Tokyo, Japan; [6]Department of Physiology, Keio University School of Medicine, Tokyo, Japan; [7]Division of Hematology and Rheumatology, Department of Internal Medicine, Kinki University Faculty of Medicine, Osaka, Japan; [8]Department of Pediatrics, Hirosaki University Graduate School of Medicine, Aomori, Japan; [9]Department of Pediatric Hematology/Oncology, The Institute of Medical Science, The University of Tokyo, Tokyo, Japan; [10]Division of Stem Cell Processing, Center for Stem Cell Biology and Regenerative Medicine, The Institute of Medical Science, The University of Tokyo, Tokyo, Japan and [11]Department of Hematology and Oncology, Division of Clinical Research, Research Institute for Radiation Biology and Medicine, Hiroshima University, Hiroshima, Japan. Correspondence: Professor H Nakajima, Division of Hematology, Department of Internal Medicine, Keio University School of Medicine, 35 Shinanomachi, Shinjuku-ku, Tokyo 160-8582, Japan.
E-mail: hnakajim@z2.keio.jp
[12]Present address: Department of Hematology, Juntendo University School of Medicine, Tokyo, Japan.
Received 30 October 2013; revised 30 March 2014; accepted 9 April 2014; accepted article preview online 15 April 2014; advance online publication, 13 May 2014

evident clinical symptoms or developmental abnormalities except mild thrombocytopenia from their childhood. However, approximately half of FPD/AML patients develop MDS or acute leukemia after a long latency, generally after the third decade of their lives. These facts together with insights from mouse studies[14] clearly indicate that *RUNX1* mutation *per se* is not sufficient for leukemia development, but it establishes preleukemic state that predisposes cells to full-blown leukemia by acquiring additional genetic events.[15,16] It is therefore expected that studying the pathogenesis of FPD/AML would provide a valuable insight into the molecular mechanism of leukemia or MDS with *RUNX1* mutation. However, rarity of FPD/AML pedigrees and limited opportunity to obtain their patient samples has tremendously hampered the study.

Induced pluripotent stem cells (iPSCs) provide us with novel opportunities for disease modeling and drug discovery[17,18] Hematopoietic differentiation of iPSCs can be induced by co-culture on stromal cells, and iPSC-derived hematopoietic progenitors can be used further for recapitulating disease phenotypes.[19–27] As iPSCs can be an indefinite source for differentiated cells, they are particularly useful when disease samples cannot be easily obtained from patients.

To investigate the physiological function of *RUNX1* in human hematopoiesis and the pathophysiology of FPD/AML, we derived iPSCs from three distinct FPD/AML pedigrees (FPD-iPSCs) and examined their defects in the emergence of hematopoietic progenitor cells (HPCs) and hematopoietic differentiation. These pedigrees have distinct heterozygous mutations in *RUNX1* gene, two in the N-terminal RUNT domain affecting its DNA-binding activity and one in the C-terminal region affecting its transactivation capacity. Three FPD-iPSC lines uniformly presented a variety of defects in the emergence in HPCs and MgK differentiation, which were rescued by overexpression of WT-*RUNX1*. We further demonstrated that overexpression of mutant-*RUNX1* in WT-iPSCs did not recapitulate the phenotype of FPD-iPSCs, showing that the mutations were of loss-of-function type. Taken together, this study, for the first time, demonstrated that haploinsufficient *RUNX1* allele imposed cell-intrinsic defects on the emergence of HPCs and MgK differentiation in human experimental settings and revealed differential impacts of *RUNX1* dosage on human and murine megakaryopoiesis.

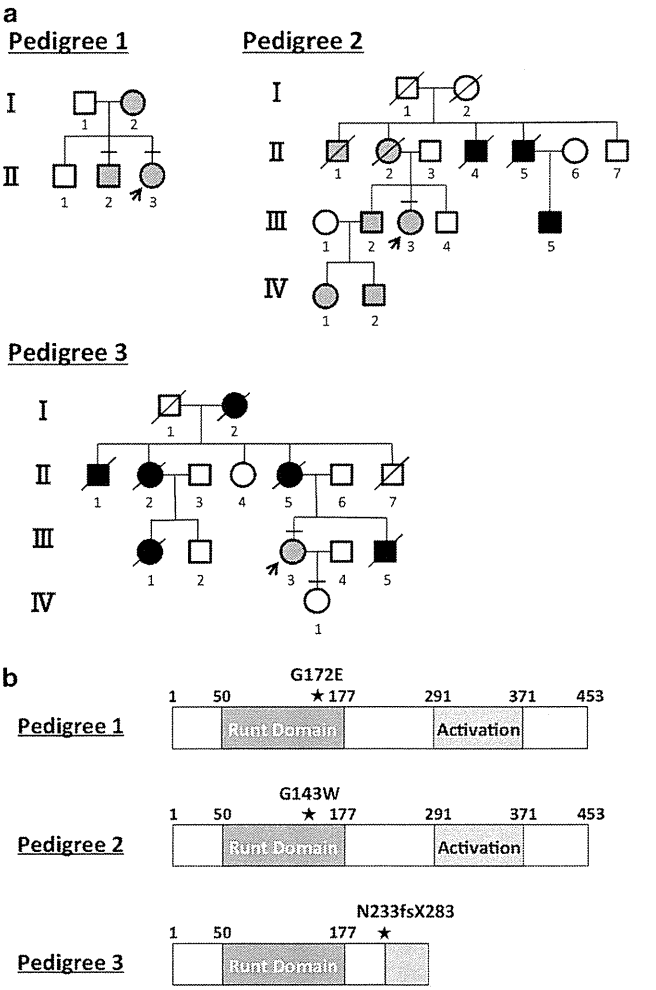

Figure 1. Pedigrees of FPD/AML and sequence analysis of *RUNX1* gene. (**a**) Family trees of three FPD/AML pedigrees. Open symbols, unaffected individuals; gray symbols, patients with thrombocytopenia; black symbols, patients who developed acute leukemia or MDS. Slash lines represent deceased individuals. Arrows denote patients enrolled in the study. (**b**) Summary of *RUNX1* mutations identified in FPD/AML pedigrees. Amino acid numbers are shown on the top of each panel. Positions of mutated amino acids are shown in filled stars. An area with oblique lines denotes irrelevant amino-acid sequence added due to a frame-shift mutation. Activation; transactivation domain.

MATERIALS AND METHODS

Patients

Family trees of three FPD/AML pedigrees are depicted in Figure 1a. Peripheral blood samples from affected patients were collected after obtaining written informed consent. The study was conducted with approval from the internal review board of Keio University School of Medicine, Tokyo, Japan and conformed to the principles outlined in the Declaration of Helsinki for use of human tissue or subjects.

DNA sequence

Genomic DNA was purified by phenol–chloroform method or by QIAamp DNA Micro Kit (Qiagen, Tokyo, Japan) according to the manufacturer's protocol. RUNX1 mutations of iPSCs were verified by direct sequencing of PCR product of *RUNX1* gene amplified from genomic DNA of iPSCs. PCR was performed by PicoMaxx high-fidelity PCR system (Agilent Technologies, Santa Clara, CA, USA) with primers for *RUNX1* that were previously described.[3] PCR products were purified and subjected to direct sequencing by using BigDye Terminator v1.1 Cycle sequencing kit (Life Technologies Japan, Tokyo, Japan) and ABI Prism 310 Genetic Analyzer (Life Technologies Japan).

Generation of iPSCs and cell culture

iPSCs were established from peripheral T cells obtained from patients. Detailed protocol for generating iPSCs from human peripheral blood mononuclear cells was previously described.[28] Control iPSCs were generated from peripheral T cells of healthy male donors after informed consent. Established iPSCs were maintained on inactivated mouse embryonic fibroblasts in iPSC medium, and cells were passaged by treating cells with 1 mg/ml collagenase IV (Life Technologies Japan) every 5–6 days.

Reverse transcription-PCR (RT-PCR)

Total RNA was isolated using TRIZOL reagent (Life Technologies Japan) according to the manufacturer's instructions. cDNA was reverse-transcribed using SuperScript II reverse transcriptase (Life Technologies Japan). PCR was performed using PicoMaxx high-fidelity PCR system (Agilent Technologies) as previously described.[29] Quantitative RT-PCR (qRT-PCR) was performed as previously described.[29] Primer sequences are listed in Supplementary Table S1.

Teratoma formation assay

iPSCs (1×10^7) were injected into the testis of NOD-SCID mice (CLEA Japan, Tokyo, Japan) under anesthesia with pentobarbital sodium (Kyoritsu Seiyaku Corporation, Tokyo, Japan). Eleven weeks after injection, tumors were dissected and fixed in 4% paraformaldehyde in phosphate-buffered-

saline. Fixed tissues were then embedded in paraffin, sectioned and stained with hematoxylin and eosin for analysis.

Immunofluorescence staining

Immunofluorescence staining was performed using the following primary antibodies: anti-NANOG (Abcam, Cambridge, MA, USA), anti-OCT3/4 (Santa Cruz Biotechnology, Dallas, TX, USA), anti-SSEA 3 (Millipore, Billerica, MA, USA), anti-SSEA 4 (Millipore), anti-Tra1-60 (Millipore), and anti-Tra1-81 (Millipore). The secondary antibodies used were: anti-mouse immunoglobulin G (IgG), anti-mouse IgM, anti-rabbit IgG, and anti-rat IgM monoclonal antibodies conjugated with Alexa Fluor 488 or 594 (Life Technologies Japan). Fluorescent images were captured using fluorescence microscope (IX70, Olympus, Tokyo, Japan) with CCD camera (DP70, Olympus).

Hematopoietic differentiation of iPSCs

We used AGM-S3 co-culture [3031] or embryonic stem (ES) sac protocols[32] to assess hematopoietic differentiation of iPSCs as previously described. For AGM-S3 co-culture, iPSCs were plated onto inactivated AGM-S3 cells and cultured for 2–3 days with iPSC medium. On day 2 or 3, medium was replaced with Iscove's modified Dulbecco's medium (Sigma, St Louis, MO, USA) supplemented with 10% fetal bovine serum (Sigma), 20 ng/ml human vascular endothelial growth factor (PeproTech, Rocky Hill, NJ, USA), 1% nonessential amino acid solution (Life Technologies Japan), 100 μM 2-ME (Wako, Osaka, Japan) and 1 mM L-glutamine (Wako). Hematopoietic cells recognized as 'cobble-stone' area surrounding iPS colonies emerge on day 10–14 of co-culture, which are then harvested using 0.05% trypsin/EDTA (Wako) for further experiments.

For ES sac formation, small iPS colonies were transferred onto irradiated C3H10T1/2 cells and co-cultured in Iscove's modified Dulbecco's mediu supplemented with 15% fetal bovine serum, 10 μg/ml human insulin, 5.5 μg/ml human transferrin, 5 ng/ml sodium selenite (Sigma), 2 mM L-glutamine (Life Technologies Japan), 0.45 mM α-monothioglycerol (Sigma), 50 μg/ml ascorbic acid (Sigma) and 20 ng/ml human vascular endothelial growth factor. On days 14 – 15 of culture, sac-like structure containing hematopoietic cells (iPS-sac) formed on the feeders were manually collected into 50-ml tubes, gently crushed with pipetting and passed through a 40-μm cell strainer to obtain hematopoietic progenitors.

Colony-forming assay

$CD34^+$ cells derived from iPSCs by AGM-S3 co-culture were sorted by flow cytometry and subjected to colony-forming assays using Methocult H4435 (Stem Cell Technologies, Vancouver, BC, Canada). Numbers and types of colonies were assessed on day 14.

Flow cytometry

Cells were stained in phosphate-buffered-saline/5% fetal bovine serum with the following monoclonal antibodies: anti-CD34-fluorescein isothiocyanate (FITC), anti-CD45-phycoerythrin (PE), anti-CD31-PE, anti-CD41a-PE, anti-CD42b-FITC (BD Pharmingen, San Jose, CA, USA), anti-glycophorin A (GPA)-FITC and anti-CD43- allophycocyanin (BioLegend, San Diego, CA, USA). Stained cells were analyzed by fluorescence-activated cell sorting (FACS) Calibur with the CellQuest software (BD Biosciences, San Jose, CA, USA) or sorted by MoFlo (Beckman Coulter, Brea, CA, USA). The data were analyzed by the FlowJo software (Tomy Digital Biology, Tokyo, Japan).

Differentiation of MgKs from $CD34^+$ cells

$CD34^+$ cells generated from iPSCs were sorted by flow cytometry and cultured in minimum essential medium alpha (Life Technologies Japan) supplemented with 10% bovine serum albumin, 100 μM 2-ME, 100 ng/ml stem cell factor (PeproTech) and 10 ng/ml thrombopoietin (PeproTech) at 37 °C under hypoxia condition (5% O_2). After 3 days of culture, cells were counted, harvested and analyzed by flow cytometry.

Stable transfection of iPSCs

pcDNA3.1/Flag-WT-*RUNX1* expressing human WT-*RUNX1b* isoform, pcDNA3.1/Flag-*RUNX1*^{G172E} or pcDNA3.1/*RUNX1*^{N233fsX283} was transfected into iPSCs using FuGENE HD transfection reagent (Promega, Madison, WI, USA) according to the manufacturer's protocol. After 2 days of transfection, stable transformants were selected in human ES medium supplemented with 100 μg/ml of G418 (Roche, Basel, Switzerland). Surviving colonies were picked up around day 14 of selection and subjected to further analyses of mRNA and protein expression.

Western blotting

Preparation of protein extracts and western blotting were performed as previously described.[33] Briefly, iPSCs were lysed in the lysis buffer (1% Nonidet P-40; 20 mM Tris-HCl, PH7.5; 150 mM NaCl; 1 mM phenylmethylsulfonyl floride; 1 μg/ml leupeptin). Proteins were separated by sodium dodecyl sulfate-polyacrylamide gel electrophoresis and transferred to PROTRAN BA85 membrane (Schleicher and Schuell, Dassel, Germany). Membranes were blocked with 5% non-fat milk in TBS-T (0.1% Tween-20) and hybridized with anti-FLAG M2 antibody (Sigma), anti-RUNX1 rabbit polyclonal antibody (gift from H Harada) or anti-α-tubulin monoclonal antibody (Sigma) followed by a horseradish peroxidase-conjugated anti-mouse or anti-rabbit immunoglobulin G secondary antibody (GE Healthcare, Pittsburgh, PA, USA). Bound antibodies were detected by enhanced chemiluminescence (GE Healthcare).

Statistical analysis

All statistical analyses were performed using unpaired Student's *t*-test. *P*-values < 0.05 were considered statistically significant.

RESULTS

Derivation of iPSCs from patients with FPD/AML

In order to investigate the physiological function of *RUNX1* in human hematopoiesis and the pathophysiology of FPD/AML, we derived iPSCs from three distinct FPD/AML pedigrees to examine their defects in the emergence of blood cells and hematopoietic differentiation. Three FPD/AML pedigrees that we utilized in the study are depicted in Figure 1a. These pedigrees carried distinct heterozygous mutations in *RUNX1* gene, two in the N-terminal RUNT domain and one in the C-terminal region (Figure 1b). N-terminal mutations in RUNT domain in pedigrees 1 and 2 (G172E and G143W) were considered to affect DNA-binding activity of RUNX1, and C-terminal mutation in pedigree 3 (N233fsX283) was reported to abrogate the transactivation/ repression capacity.

After obtaining informed consent from the affected patients, we established iPSCs from their peripheral T cells by infecting Sendai viruses expressing four reprogramming factors (*OCT3/4*, *SOX2*, *KLF4* and *c-MYC*) (Figure 2a).[34] FPD-iPSCs could be established in comparable frequency as the one from normal individuals (WT-iPSCs), and their behavior in the culture and the morphology of the colonies were indistinguishable from those of WT-iPSCs (Figure 2b). We confirmed that each iPSCs harbored the same *RUNX1* mutation identified in somatic cells of the original patients (Figure 2c). Initial characterization of FPD-iPSCs revealed that the established clones retained typical characteristics of pluripotent stem cells such as the expression of immature ES cell markers (for example, Nanog, Oct3/4, SSEA-3, SSEA-4, Tra-1-60 or Tra-1-81) as examined by immunostaining (Figure 2d), RT-PCR (Figure 2e), qRT-PCR (Supplementary Figure S1a) or flow cytometry (Supplementary Figure S1b) and the ability to form teratomas with differentiation to three germ layers in immunodeficient mice (Figure 2f). Sendai virus-induced reprogramming does not accompany viral integration into the host genome, and we confirmed that the transduced genes were not expressed on mRNA level in the established FPD-iPSC clones (Figure 2e).

Defective emergence of hematopoietic progenitors from FPD-iPSCs

To investigate the impact of *RUNX1* mutation on the emergence of hematopoietic progenitors (HPCs), we induced hematopoietic differentiation of FPD-iPSCs by co-culture on AGM-S3 cells, a stromal cell line established from aorta–gonad–mesonephros (AGM) region[21,35] (Figure 3a). Briefly, WT-iPSCs and FPD-iPSCs were dispersed and plated on inactivated AGM-S3 cells and were co-cultured in the presence of vascular endothelial growth factor.

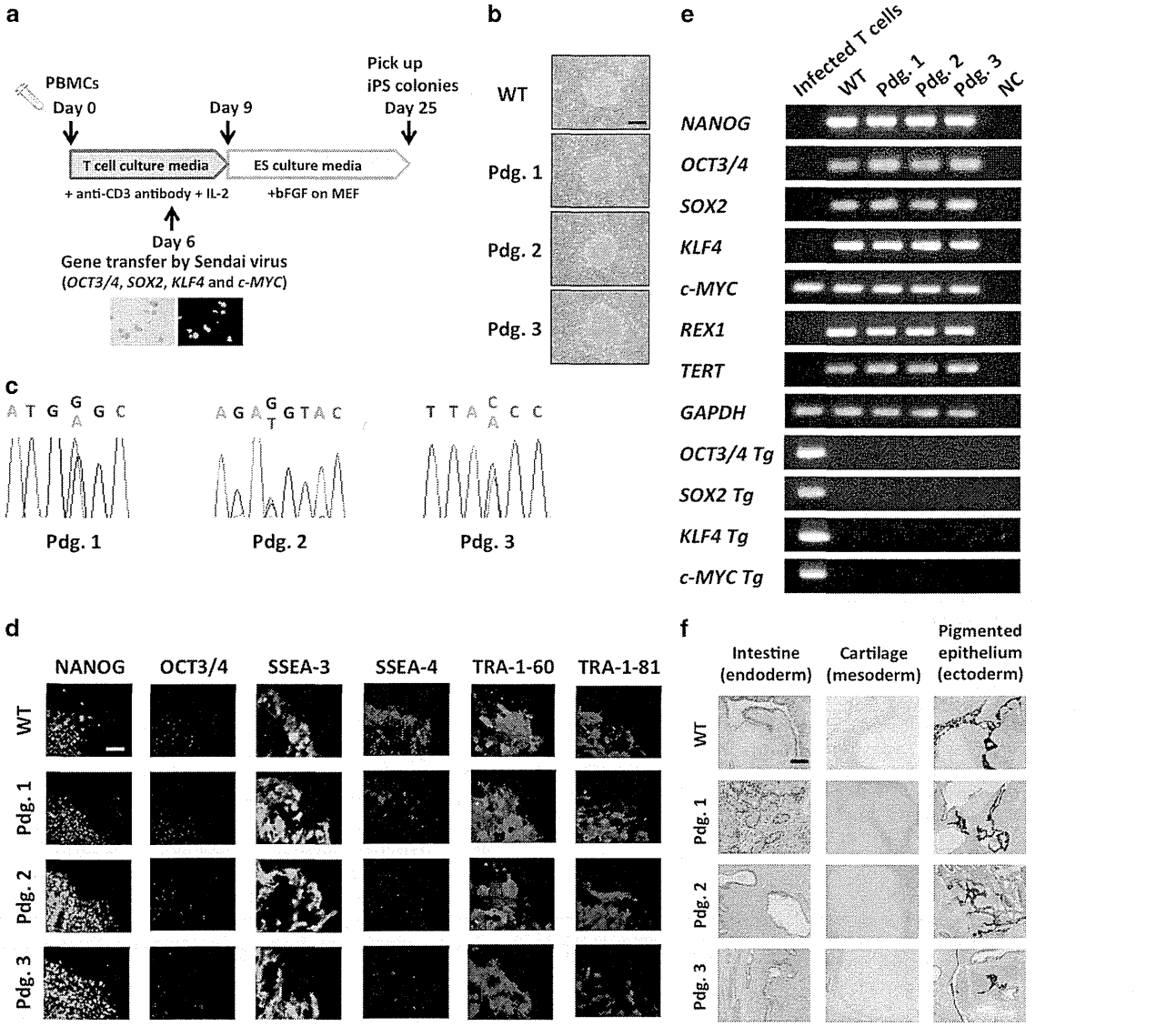

Figure 2. Generation and characterization of iPSCs from FPD/AML patients. (**a**) Schematic diagrams of iPSC derivation from FPD/AML patients using terminally differentiated peripheral T cells. Pictures are T cells infected with control retrovirus expressing green fluorescent protein (GFP) (left; light microscope, right; GFP). (**b**) Morphology of the colonies of WT-iPSCs or FPD-iPSCs. Scale bar = 500 μm. Pdg.; pedigree. (**c**) *RUNX1* mutations in FPD-iPSCs. Each FPD-iPSC retained the same mutation as somatic cells of the original patient. (**d**) Immunofluorescence staining for human embryonic stem cell (hESC) markers. Scale bar = 200 μm. (**e**) RT-PCR analysis for the endogenous hESC maker genes (*NANOG*, *OCT3/4*, *SOX2*, *KLF4*, *c-MYC*, *REX1* and *TERT*), and SeV-transgenes (*OCT3/4 Tg*, *SOX2 Tg*, *KLF4 Tg* and *c-MYC Tg*). NC; negative control. Infected T cells represent T cells 3 days after SeV infection. (**f**) Teratoma formation assay. iPSCs were injected into the testes of NOD-SCID mice. Teratomas were resected, fixed, sectioned and stained with hematoxylin–eosin. WT-iPSC and all FPD-iPSCs showed differentiation to three germ layers, including pigmented epithelium (ectoderm), cartilage (mesoderm) and intestinal glandular structure (endoderm). Scale bar = 50 μm.

On day 15 or day 16 of culture, cells were collected and analyzed for the emergence of HPCs by flow cytometry. Interestingly, the frequencies of $CD34^+$ and $CD45^+$ cells emerged from FPD-iPSCs were decreased to about 40–60% and 20–40% of WT-iPSCs, respectively, suggesting that HPC emergence was profoundly impaired by *RUNX1* mutation (Figures 3b and c). Notably, these defects were observed to a similar extent in all three FPD-iPSC lines, showing that either N-terminal or C-terminal mutations of *RUNX1* do not make any differential effects on the emergence of $CD34^+$ and $CD45^+$ cells. In contrast, expression of CD235a/GPA, an early erthroid-MgK specification marker during human ES cell differentiation,[36] was not impaired in all three FPD-iPSCs as compared with WT (Figure 3c), which suggests that the emergence of early erthroid-MgK progenitors from iPSCs was not affected by *RUNX1* mutation.

In order to quantitatively evaluate the frequency of lineage-committed HPCs derived from each FPD-iPSC, $CD34^+$ cells generated by AGM-S3 co-culture were sorted by flow cytometry and subjected to colony-forming assays. As shown in Figure 3d, the frequencies of granulocyte-monocyte (GM), erythroid (E) or mix colony-forming-cells (CFCs) in $CD34^+$ fraction were significantly lower in FPD-iPSCs as compared with those of WT. It is of note that differences in size and morphology of the colonies were not discernible between WT- and FPD-iPSCs (Supplementary Figure S2).

To examine the HPC emergence in more detail, we undertook ES-sac differentiation protocol to induce hematopoietic differentiation.[32]

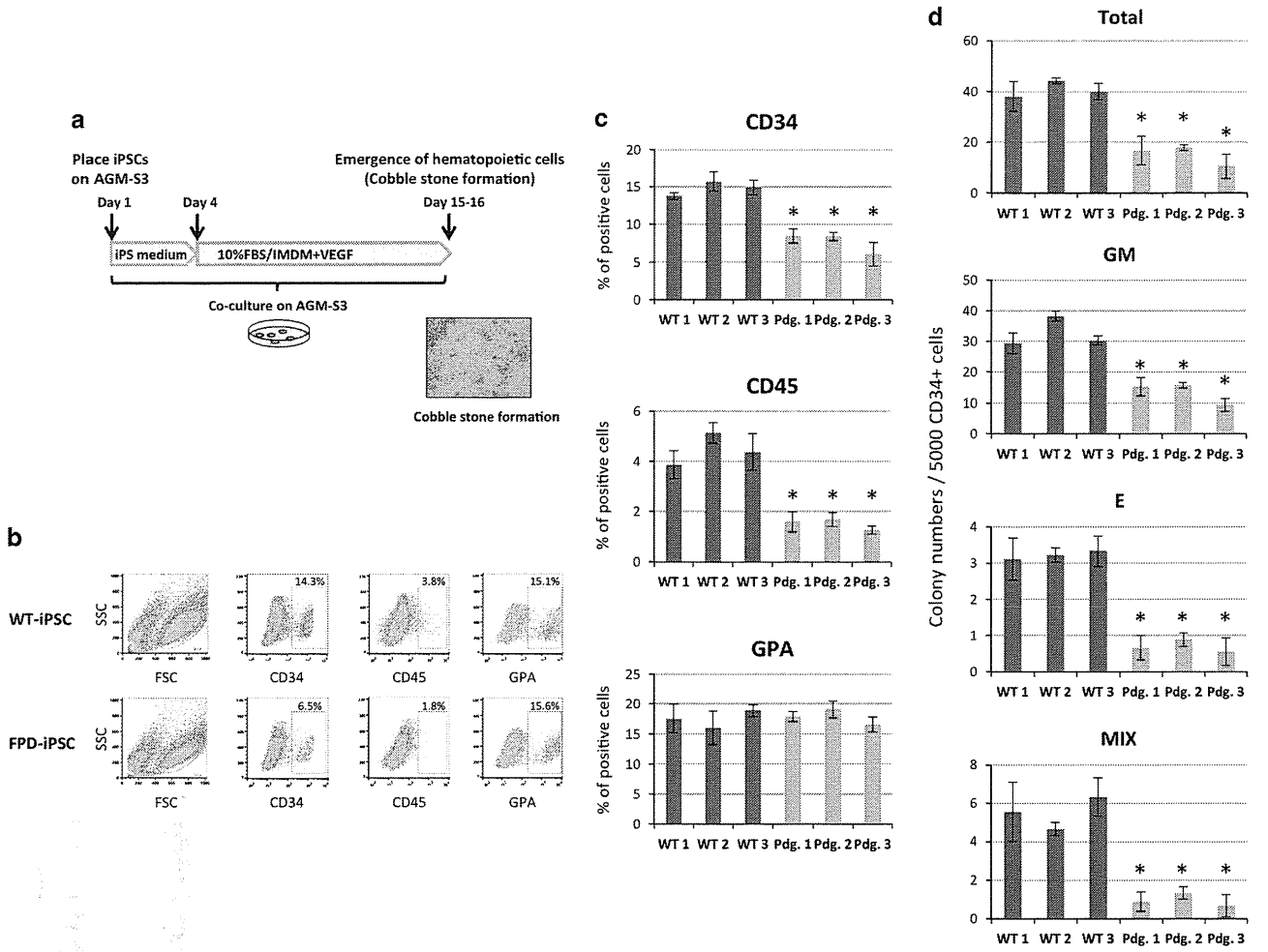

Figure 3. Hematopoietic differentiation of iPSCs by AGM-S3 co-culture. (**a**) Schematic diagram of hematopoietic differentiation of iPSCs by co-culture with AGM-S3. Photograph on the right shows a cobblestone area that appeared around iPSC colonies on day 13. (**b**) Representative flow cytometric profile of cells harvested from AGM-S3 co-cultures. Analyses of WT-iPSC (WT1) and FPD-iPSCs (Pdg. 1) are shown. Mononuclear cell (MNC) fractions were gated and analyzed for CD34, CD45 and GPA. (**c**) Percentages of $CD34^+$, $CD45^+$ or GPA^+ cells against MNCs are shown ($n=3$, mean ± s.d.). All FPD-iPSCs uniformly showed impaired differentiation to CD34 or CD45 cells, while differentiation of GPA^+ cells remained intact. WT1, WT2 and WT3 represent WT-iPSCs, established from three distinct individuals. $^*P<0.01$. (**d**) Sorted $CD34^+$ cells (5000 cells/ plate) from AGM-S3 co-culture were subjected to colony-forming assay as described in Methods. GM, CFU-GM; E, BFU-E; Mix, CFU-mix. Data are shown as mean ± s.d. ($n=3$). $^*P<0.01$.

The efficiency of ES-sac induction was comparable between WT- and FPD-iPSCs (Supplementary Figure S3a). As shown in Figures 4a–c and Supplementary Figure 3b, the percentage of $CD34^+CD43^+CD45^-$ cells, earliest HPCs detected during ES cell/iPSC differentiation (HP1), was decreased to 10–40% of WT in FPD-iPSCs.[36,37] Furthermore, $CD34^+CD43^+CD45^+$ or $CD34^-CD43^+CD45^+$ cells, representing late-committed HPCs (HP2) or myeloid-restricted HPCs (Lin P), respectively, were drastically decreased to 3–5% of WT in FPD-iPSCs (Figure 4c). Notably, these frequencies were not statistically different between FPD-iPSCs with N-terminal *RUNX1* mutation (FPD-N-iPSCs) (pedigree 1 and pedigree 2) and those with C-terminal *RUNX1* mutation (FPD-C-iPSCs) (pedigree 3) in this assay. We have also checked the frequency of various lineage-committed progenitors in the fixed number of $CD34^+CD43^+CD45^-$ cells by colony-forming assays. This revealed that the frequencies of GM-, E- and mix-CFCs in $CD34^+CD43^+CD45^-$ cells were comparable between WT- and FPD-iPSCs (Supplementary Figure S3c), and no apparent difference was noted in the morphology of the colonies (Supplementary Figure S3d).

Taken together, these results clearly indicate that the net emergence of HPCs from human iPSCs is profoundly impaired by *RUNX1* mutation.

Defective differentiation and maturation of MgKs from FPD-iPSCs

It has been shown that *RUNX1* was critical for MgK differentiation and maturation by gene-disruption studies in mice.[1] We asked whether this finding could be applied to human settings by using FPD-iPSC-differentiation model. To do this, $CD34^+$ cells induced in AGM-S3 co-culture system were assessed for their ability to differentiate into MgKs in liquid culture with thrombopoietin and SCF (Figure 5a). Interestingly, $CD34^+$ cells from FPD-iPSCs generated $CD41a^+$ MgKs in significantly lower frequencies (30–50%) as compared with WT in this assay (Figures 5b and d). Actual number of MgKs generated from $CD34^+$ cells was also decreased in the FPD-iPSC-group as compared with WT (Supplementary Figure S4). Of note, MgKs differentiated from FPD-iPSCs were less mature and smaller in size as evidenced by CD42b and mean-forward scatter (FSC), respectively, by flow cytometry (Figure 5d). However, differences in size or morphology were not readily apparent by cytospin preparation (Figure 5c).

These results indicate that differentiation of MgKs is impaired both quantitatively and qualitatively in FPD-iPSCs. Again, all three FPD-iPSC lines shared the same phenotype in these assays, suggesting that N-terminal and C-terminal *RUNX1* mutations

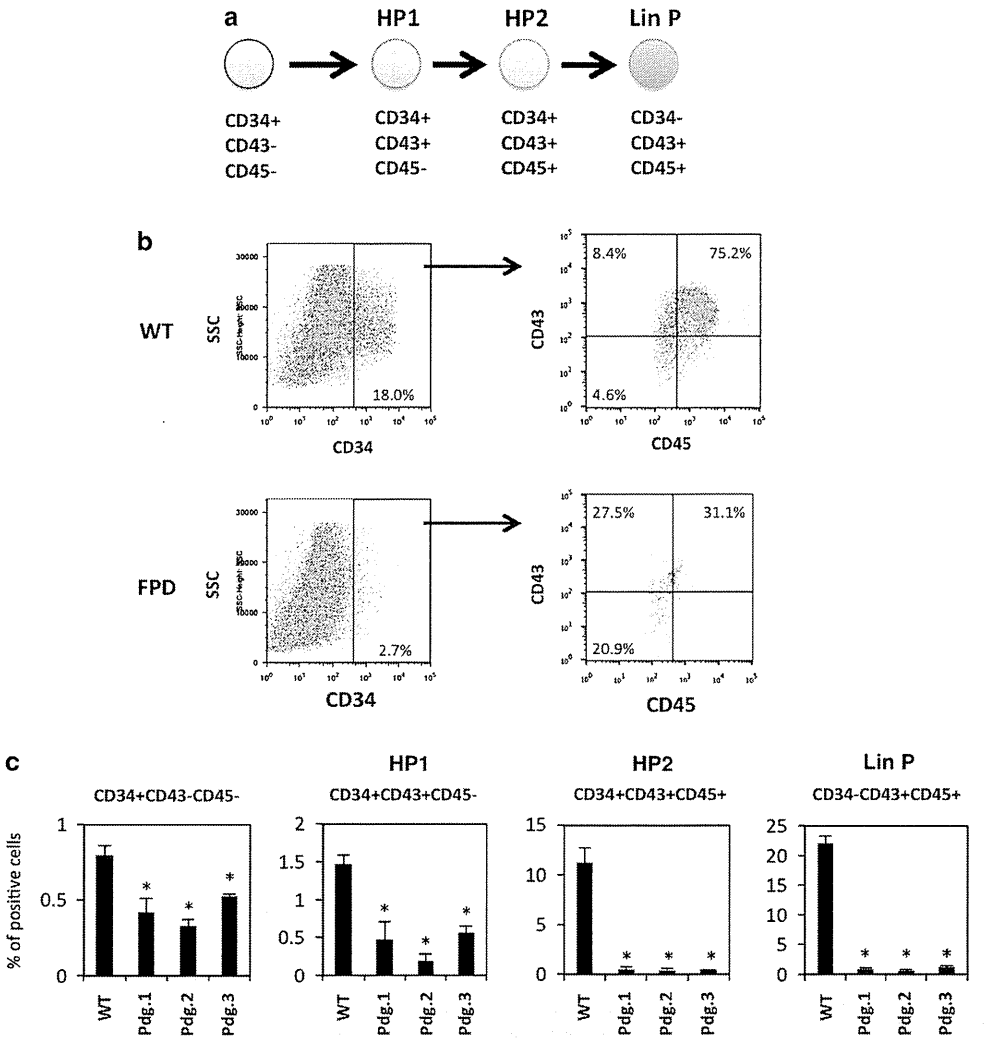

Figure 4. Emergence of hematopoietic progenitors from iPSCs. (**a**) A model of hematopoietic differentiation from human ES cells.[36] HP1, early HPC; HP2, late-committed HPC; Lin P, myeloid-restricted HPC. (**b**) Representative flow cytometric profiles of HPCs generated from WT- or FPD-iPSCs by ES-sac protocol. (**c**) Percentages of HPCs generated from WT- or FPD-iPSCs analyzed by flow cytometry. Data are mean ± s.d. ($n = 3$). $^*P < 0.01$. SSC, side scatter.

impose similar defects in MgK differentiation and maturation in FPD-iPSCs.

Phenotypic rescue of FPD-iPSCs by overexpression of WT *RUNX1*

As mutant *RUNX1* has been reported to act in a loss-of-function or dominant-negative manner for WT-*RUNX1*, we tried to rescue the phenotypes of FPD-iPSCs by overexpressing WT-*RUNX1*. FPD-N-iPSC and FPD-C-iPSC clones (pedigrees 1 and 3) overexpressing WT-*RUNX1* were established by transfecting the vector expressing Flag-tagged WT-*RUNX1*. Three clones for each FPD-iPSC were established, and they presented highly similar phenotype. The expression of Flag-RUNX1 was confirmed by western blotting and RT-PCR (Figures 6a and b). FPD-iPSCs overexpressing Flag-*RUNX1* was morphologically indistinguishable from parental FPD-iPSCs, and their immature phenotype was confirmed by the expression of pluripotent genes such as *NANOG* or *OCT3/4* by RT-PCR (Figure 6b). We then investigated whether these established clones recovered the capacity to differentiate into hematopoietic lineage. As expected, overexpressing WT-*RUNX1* in FPD-iPSCs rescued the emergence of $CD34^+$ and $CD45^+$ cells by AGM-S3 co-culture both in FPD-N-iPSC (pdg. 1) and FPD-C-iPSC (pdg. 3), whereas mock control did not (Figure 6c). Moreover, CFC numbers (CFU-GM, CFU-E, CFU-mix) in $CD34^+$ cells and differentiation of MgKs as examined by CD41a expression and cell numbers were also rescued by WT-*RUNX1* overexpression (Figures 6d and e, Supplementary Figure S5). Morphology of the colonies was not different between parental FPD-iPSC and mock- or Flag-*RUNX1*-transfected FPD-iPSCs (Supplementary Figure S6). Interestingly, however, mean-FSC by flow cytometry was not recovered, and CD42 expression was rescued only in pedigree 3 (Figure 6e). This suggests that overexpression of WT-*RUNX1* only partially rescues Mgk maturation. Of note, RT-PCR analysis showed that the transgene for WT-*RUNX1* was not silenced either before or after the induction of HPCs (Supplementary Figure S7).

Taken together, these results support the notion that mutant *RUNX1* in FPD/AML acts in a loss-of-function or dominant-negative manner to the WT allele in hematopoietic differentiation, although some aspects of impaired Mgk maturation in FPD-iPSCs may not be the consequence of impaired *RUNX1* function.

Expression of RUNX1 target genes in FPD-iPSC-derived HPCs

To obtain clues whether mutant *RUNX1* acts in a loss-of-function or dominant-negative manner in hematopoietic differentiation,

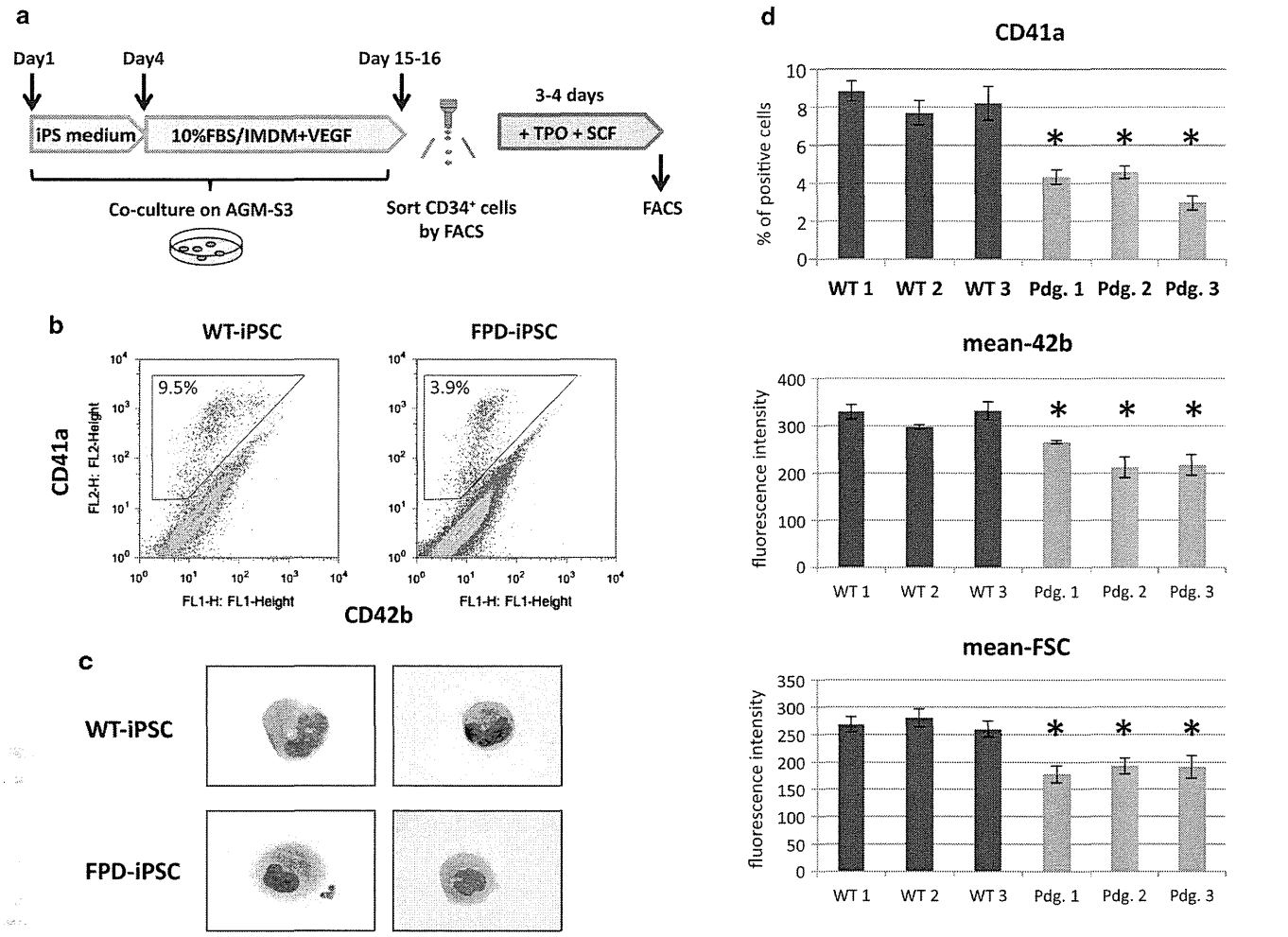

Figure 5. Differentiation of MgKs from iPSC-derived CD34$^+$ cells. (**a**) Schematic diagram of MgK differentiation from iPSC-derived CD34$^+$ cells. CD34$^+$ cells from AGM-S3 co-culture were sorted and cultured in MgK differentiation medium containing thrombopoietin and stem cell factor. Cells were harvested and analyzed on day 3 or 4. (**b**) Representative FACS profile of MgKs generated from iPSC-derived CD34$^+$ cells. Analyses of WT-iPSC (WT1) and FPD-iPSCs (Pdg. 1) are shown. (**c**) Morphology of MgKs derived from WT-iPSC (WT1) and FPD-iPSCs (Pdg. 1) (Giemsa staining. Original magnification; × 1000). (**d**) Percentage of CD41a$^+$ cells, mean fluorescence intensity of CD42b and mean-FSC of WT-iPSC- or FPD-iPSC-derived Mgks are shown. Data are mean ± s.d. ($n = 3$). *$P < 0.01$.

we examined the expression of *RUNX1* target genes by qRT-PCR in hematopoietic cells derived from FPD-iPSCs. Interestingly, expressions of well-known *RUNX1* target genes such as *PU.1*, GM-colony stimulating factor (*GM-CSF*) or myeloperoxidase (*MPO*)[38] in FPD-iPSC-derived hematopoietic cells were decreased to approximately half of those of WT (Figure 7). These data strongly suggest that *RUNX1* alleles of FPD-iPSCs are haploinsufficient.

Overexpression of mutant *RUNX1* in WT-iPSCs does not recapitulate the phenotype of FPD-iPSCs

In order to gain further insight into the role of mutant *RUNX1* in hematopoietic differentiation of iPSCs, we derived WT-iPSCs overexpressing mutant *RUNX1* and examined their differentiation to hematopoietic lineage (Figure 8a). In this experiment, we tested both N-terminal G172E *RUNX1* mutant (*RUNX1*-N^m) from pedigree 1 and C-terminal N233fsX283 *RUNX1* mutant (*RUNX1*-C^m) from pedigree 3.

Three stable iPSC clones for each *RUNX1* mutant were established, and the expression of mutant RUNX1 protein in each clone was confirmed by western blotting (Figure 8a). These clones were then subjected to hematopoietic differentiation assays by AGM-S3 co-culture system. Surprisingly, both *RUNX1* mutants, either *RUNX1*-N^m or *RUNX1*-C^m, scarcely affected the differentiation of WT-iPSCs to HPCs (Figures 8b and c) or MgKs (Figure 8d) as examined by flow cytometry or colony assays, whereas FPD-iPSCs were defective in the same settings (Figures 8b–d). Of note, the expression of mutant *RUNX1* was not silenced in CD34$^+$ cells derived from iPSC clones analyzed (Supplementary Figure S8). These results clearly demonstrated that overexpression of mutant *RUNX1* in WT-iPSCs did not recapitulate the phenotype of FPD-iPSCs. Taken together with the effects of mutant *RUNX1* on the expression of target genes (Figure 7), these results strongly suggest that *RUNX1* mutants act in a loss-of-function, not dominant-negative, manner in hematopoietic differentiation of iPSCs.

DISCUSSION

Knowledge on *RUNX1* function has been mostly derived from genetically modified animals, such as knockout mice or mutant zebrafish. It was previously shown that *Runx1* has a critical role in the establishment of definitive hematopoietic stem cells during embryonic development,[39,40] and the differentiation of MgKs and lymphocytes in adult hematopoiesis.[1] Further studies have shown that *Runx1* was required for the emergence of definitive hematopoietic stem cells from the so-called 'hemogenic

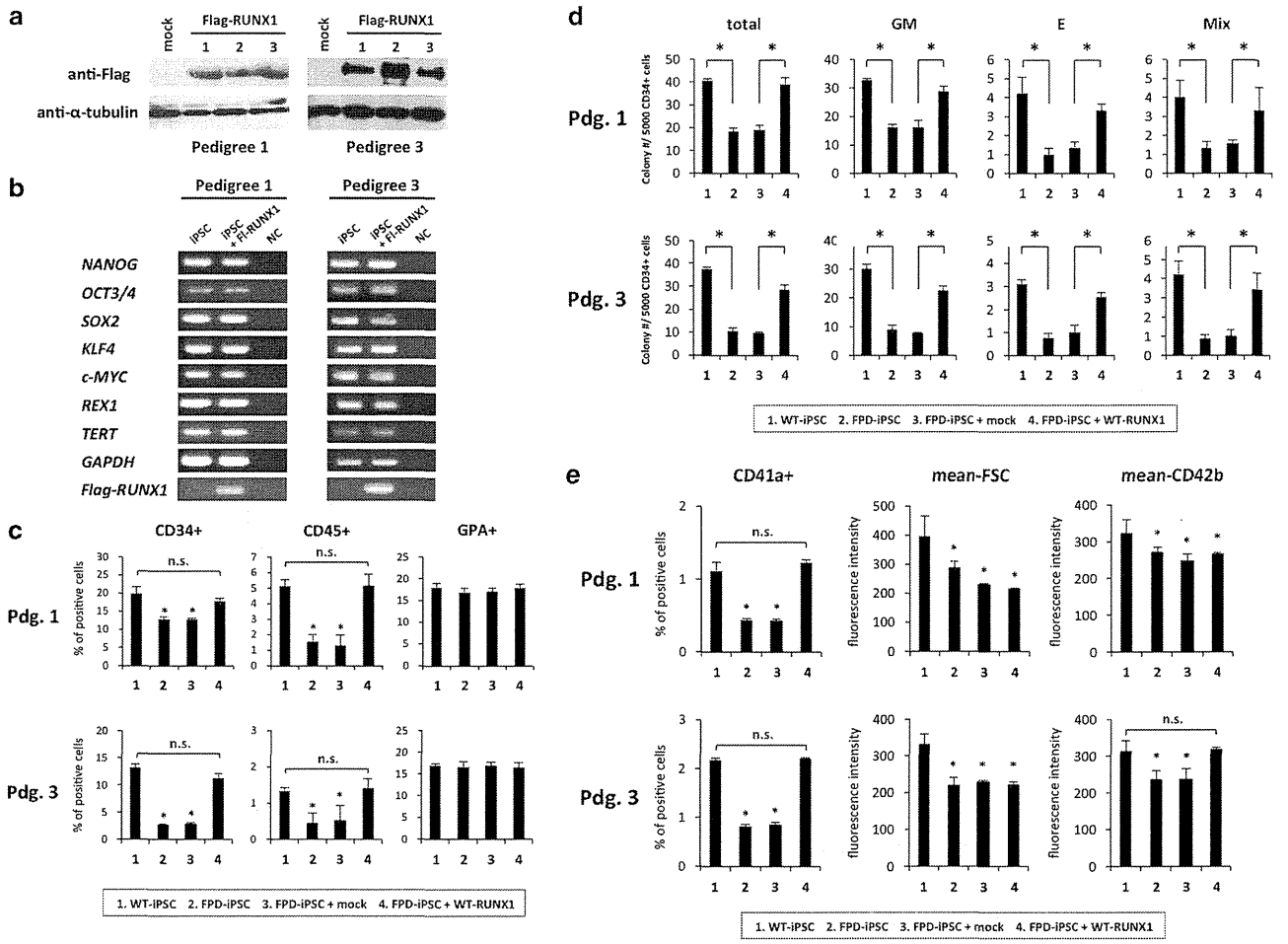

Figure 6. Phenotypic rescue of FPD-iPSCs by WT *RUNX1*. (**a**) Expression of Flag-RUNX1 protein in FPD-iPSCs transfected with pcDNA3/Flag-*RUNX1*. Three different clones were isolated for each FPD-iPSC (pedigrees 1 and 3). The clone numbers are shown on each gel. (**b**) RT-PCR analysis for the endogenous hESC maker genes and Flag-*RUNX1* before and after transfection of Flag-*RUNX1*. Fl-RUNX1, Flag-*RUNX1*; NC, negative control. (**c**) Hematopoietic differentiation of rescued FPD-iPSCs by AGM-S3 co-culture. Percentages of $CD34^+$ cells, $CD45^+$ cells and GPA^+ cells derived from each iPSC are shown. Data are mean ± s.d. ($n = 3$). *$P < 0.05$. NS, not significant. (**d**) Colony-forming assay of sorted $CD34^+$ cells. Data are mean ± s.d. ($n = 3$). *$P < 0.05$. GM, CFU-GM; E, BFU-E; Mix, CFU-mix. (**e**) Differentiation of MgKs from rescued FPD-iPSC-derived $CD34^+$ cells. Percentage of $CD41a^+$ cells, mean fluorescence intensity of CD42b and mean-FSC are shown. Data are mean ± s.d. ($n = 3$). *$P < 0.05$. NS, not significant.

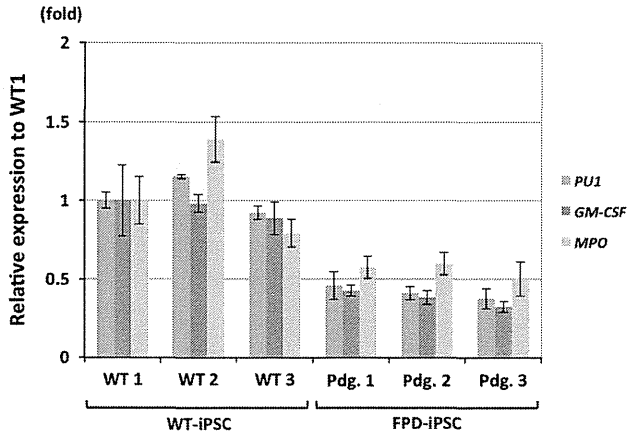

Figure 7. Expression of *RUNX1* target genes in HPCs derived from FPD-iPSCs. Cells recovered from hematopoietic colonies generated from WT- or FPD-iPSCs were subjected to RNA extraction and quantitative RT-PCR analyses for *PU.1*, *GM-CSF* or *MPO*. Data are presented as the relative expression to those of WT1 (mean ± s.d., $n = 3$).

endothelium'.[41–44] However, physiological function of *RUNX1* has been rarely investigated in human experimental settings. In order to investigate the impact of *RUNX1* mutation on human hematopoiesis and to delineate the pathophysiology of FPD/AML, we derived iPSCs from FPD/AML patients and examined their defects in hematopoietic differentiation. In this study, we, for the first time, demonstrated that human iPSCs with *RUNX1* mutation are defective in the emergence of HPCs and MgK differentiation.

We also demonstrated that mutant *RUNX1* acts in a loss-of-function manner in hematopoietic differentiation of human iPSCs, strongly suggesting that the phenotypes of FPD-iPSCs are the consequence of haploinsufficiency of *RUNX1*. This is compatible with the previous observation that significant number of FPD/AML pedigrees harbor germline heterozygous deletion of entire or a part of *RUNX1* allele. Furthermore, it was reported that genetically modified mice with heterozygous mutant *RUNX1*-knock-in (KI) alleles, which resembled human hematologic diseases, displayed 60–70% decrease of hematopoietic CFC numbers in AGM regions or FLs during murine embryogenesis, suggesting that they act as haploinsufficient alleles *in vivo*. In contrast, previous *in vitro* biochemical studies have suggested that some of the *RUNX1* mutations observed in MDS or AML act as weak dominant-negative allele.[3,9] They showed that most of the *RUNX1* mutants

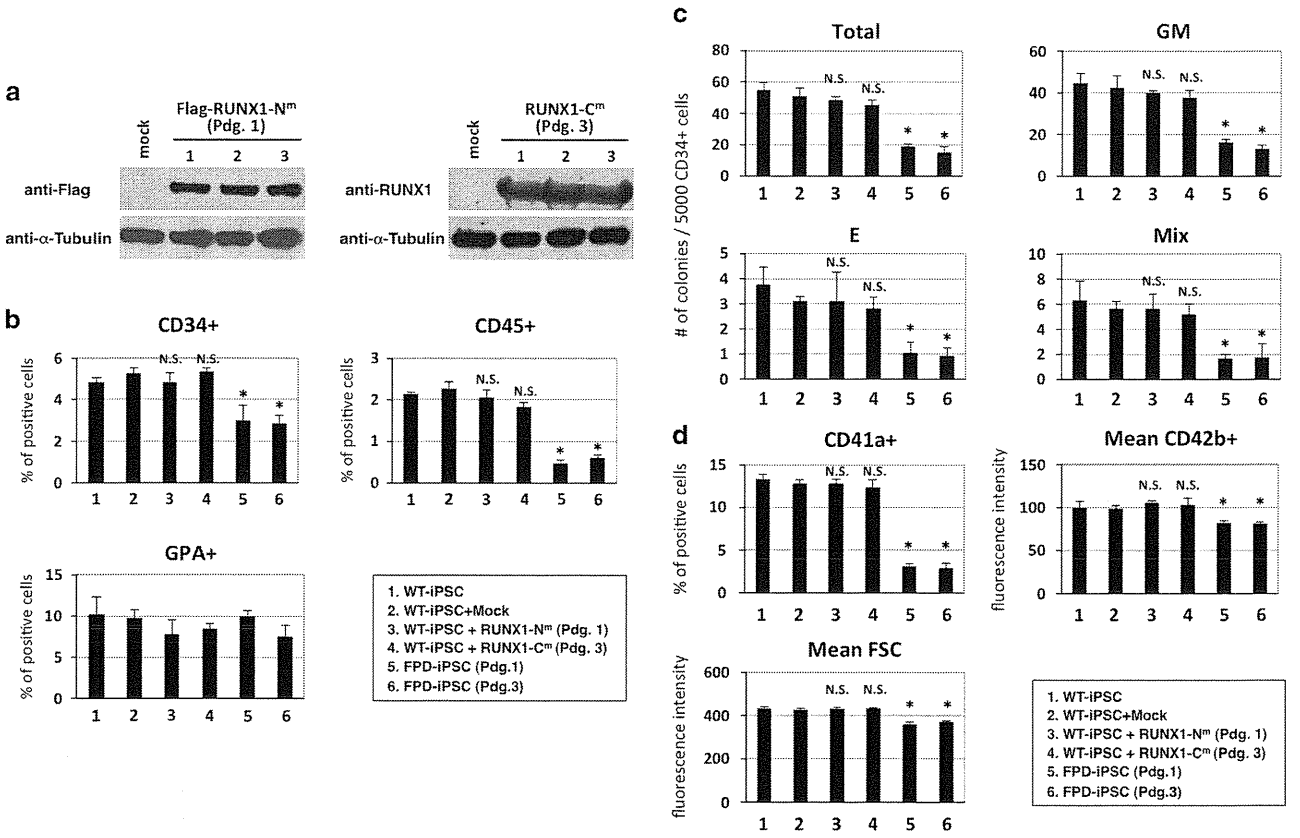

Figure 8. Effects of mutant *RUNX1* on hematopoietic differentiation of WT-iPSCs. (**a**) Expression of mutant RUNX1 protein in WT-iPSCs transfected with pcDNA3/Flag-*RUNX1*-N^m or pcDNA3/*RUNX1*-C^m. Three different clones were isolated for each *RUNX1*-mutant, and the expression of transfected genes was examined by western blotting. Flag-RUNX1-N^m and RUNX1-C^m proteins were detected by anti-Flag and anti-RUNX1 antibodies, respectively. α-Tubulin was used as a loading control. The clone numbers are shown on each lane. WT-iPSCs transfected with mock vector (mock) were used as a negative control. (**b**) Hematopoietic differentiation of WT-iPSCs expressing *RUNX1*-N^m and *RUNX1*-C^m by AGM-S3 co-culture. Cells were co-cultured on AGM-S3 cells for 10–14 days and subjected to FACS analyses. Frequencies (%) of CD34$^+$, CD45$^+$ or GPA$^+$ cells derived from WT-iPSCs expressing *RUNX1*-N^m and *RUNX1*-C^m or FPD-iPSCs (Pdg. 1 and 3) against MNCs are shown ($n=3$, mean ± s.d.). Parental WT-iPSCs and WT-iPSCs transfected with mock vector were used as controls. *$P<0.05$. NS, not significant against 'WT-iPSCs' or 'WT-iPSCs + mock'. (**c**) Colony-forming assay of HPCs derived from WT-iPSCs expressing *RUNX1*-N^m and *RUNX1*-C^m. Sorted CD34$^+$ cells (5000 cells/plate) from AGM-S3 co-culture were subjected to the assay as described in Methods. GM, CFU-GM; E, BFU-E; Mix, CFU-mix. Data are mean ± s.d. ($n=3$). *$P<0.05$. NS, not significant against 'WT-iPSCs' or 'WT-iPSCs + mock'. Description of the columns is the same as that in panel (**b**) or (**d**). (**d**) Differentiation of MgKs from CD34$^+$ cells derived from WT-iPSCs expressing *RUNX1*-N^m and *RUNX1*-C^m. Percentage of CD41a$^+$ cells, mean fluorescence intensity of CD42b and mean-FSC are shown. Data are mean ± s.d. ($n=3$). *$P<0.05$. NS, not significant against 'WT-iPSCs' or 'WT-iPSCs + mock'.

are defective in DNA binding, dimerization with CBFβ or transactivation capacities,[3,9] and thereby suppress WT-*RUNX1* by varying degrees when they are overexpressed *in vitro*.[3] Taken together, it is plausible that the effects of mutant *RUNX1* on hematopoiesis significantly vary depending on the expression levels and the cellular context. This notion is supported by the previous observation that retroviral overexpression of mutant *Runx1* in BM cells leads to the development of MDS/AML in mice, while heterozygous mutant *Runx1*-KI mice do not develop leukemia during their lifetime. Further investigation is required to reveal precise molecular mechanism for differential effect of *RUNX1* under various conditions.

Ran *et al.*[45] have recently reported that enforced expression of *RUNX1a*, a naturally occurring isoform lacking C-terminal activation/repression domain, enhanced the production of CD34$^+$CD45$^+$ HPCs from human ESCs/iPSCs, which are transplantable to immune-deficient mice. However, in our hands, overexpression of *RUNX1*^{N233fsX283} mutant (*RUNX1*-C^m), which closely resembles *RUNX1a*, in WT-iPSCs did not affect the differentiation to CD34$^+$ cells. This discrepancy could be due to a slight difference between the sequences of *RUNX1a* and *RUNX1*-C^m, the different strategies taken to deliver *RUNX1* mutants into iPSCs (lentiviral transduction vs plasmid overexpression), integration sites of the transduced gene or different iPSC clones utilized. This is certainly another issue of future investigation.

Another critical finding of this study is a cell-autonomous effect of *RUNX1* mutation on hematopoiesis. Although previous studies using mutant mice or patient samples suggested cell-autonomous effects of mutant *RUNX1* on HPC emergence and MgK differentiation, it has still been possible that extrinsic factors such as altered microenvironmental cues affected the differentiation process *in vivo*. This study demonstrated that FPD-iPSCs were defective in hematopoietic differentiation in *in vitro* assays, showing that disease-specific *RUNX1* mutation impaired the emergence of HPCs and MgK differentiation indeed in a cell-autonomous manner.

It is noteworthy that functional roles of mutant *RUNX1* on MgK differentiation and platelet production are critically different between humans and mice. In mice, heterozygous DNA-binding *Runx1* mutation never led to thrombocytopenia, and only homozygous animals presented mild MgK/platelet defects.[9] In contrast, heterozygous *RUNX1* mutation is sufficient to cause MgK defects in human settings as demonstrated by the current study. These differences could be due to a differential sensitivity of MgK

differentiation and platelet production to *RUNX1* dosage in human or mouse hematopoiesis. Molecular mechanism underlying this discrepancy definitely requires further investigation.

In MgK differentiation assays, mean-FSC by flow cytometry was significantly lower in MgKs derived from FPD-iPSCs as compared with those from WT-iPSCs, suggesting that FPD-iPSC-derived MgKs are smaller in size. Complementation of *RUNX1* activity in FPD-iPSCs by WT-*RUNX1* rescued MgK differentiation as examined by CD41a expression. Interestingly, however, mean-FSC of FPD-iPSC-derived MgKs did not return to the level comparable to that of WT in the same experiment. These results indicated that differentiation and cell size of MgKs were differentially regulated by *RUNX1* and raise a possibility that reduced size of FPD-iPSC-derived MgKs might be the consequence of novel function acquired by mutant *RUNX1*.

We were able to analyze three FPD-iPSC lines derived from three distinct FPD/AML pedigrees. Two pedigrees carried mutation in RUNT domain that disrupts DNA binding, and the other carried frame-shift mutation resulting in premature termination before C-terminal activation/repression domain. Through our *in vitro* hematopoietic differentiation analyses, we could find no major difference between the three FPD-iPSC lines in terms of HPC emergence and MgK differentiation. These results suggest that disease-specific *RUNX1* mutations impose highly similar impact on the hematopoietic differentiation of iPSCs regardless of the sites of mutation. However, it still leaves a possibility that various *RUNX1* mutations differentially affect other aspects of hematopoiesis. Particularly, as mutant *RUNX1* is involved in the malignant transformation of hematopoietic cells, it would be intriguing to examine differential impacts of various *RUNX1* mutations on the development of AML or MDS using our FPD-iPSC models.

In summary, we have successfully established iPSCs from three distinct FPD/AML pedigrees and have shown that these FPD-iPSCs are uniformly defective in HPC emergence and MgK differentiation. This report is the first to demonstrate critical roles of *RUNX1* in hematopoiesis in human experimental settings and revealed differential impact of heterozygous mutant *RUNX1* on human and mouse MgK differentiation. We also demonstrated that the phenotypes of FPD-iPSCs are the consequence of haploinsufficiency of *RUNX1*. We expect that these FPD-iPSC lines are extremely useful as an unlimited source for human HPCs with various *RUNX1* mutations, and they will serve as a novel platform for investigating multistep leukemogenesis based on *RUNX1* mutation.

CONFLICT OF INTEREST

HO is the scientific consultant of San Bio, Inc., Eisai Co Ltd. and Daiichi Sankyo Co Ltd. HN is a founder, a member of scientific advisory board and shareholder of ReproCELL and is a scientific advisor of Megakaryon, iCELL and Shionogi & Co. The remaining authors declare no conflict of interest.

ACKNOWLEDGEMENTS

We thank excellent technical assistance by J Kawakita. We also thank S Suzuki (FACS Core Laboratory, Keio University School of Medicine) for FACS sorting, W Akamatsu and M Sato (Department of Physiology, Keio University School of Medicine) and H Nakata (Division of Cardiology, Keio University School of Medicine) for cell culture or establishment of iPSCs. This work was supported in part by a grant from the Ministry of Education, Culture, Sports, Science and Technology of Japan.

REFERENCES

1 Ichikawa M, Asai T, Saito T, Seo S, Yamazaki I, Yamagata T *et al.* AML-1 is required for megakaryocytic maturation and lymphocytic differentiation, but not for maintenance of hematopoietic stem cells in adult hematopoiesis. *Nat Med* 2004; **10**: 299–304.
2 Osato M. Point mutations in the RUNX1/AML1 gene: another actor in RUNX leukemia. *Oncogene* 2004; **23**: 4284–4296.
3 Harada H, Harada Y, Niimi H, Kyo T, Kimura A, Inaba T. High incidence of somatic mutations in the AML1/RUNX1 gene in myelodysplastic syndrome and low blast percentage myeloid leukemia with myelodysplasia. *Blood* 2004; **103**: 2316–2324.
4 Christiansen DH, Andersen MK, Pedersen-Bjergaard J. Mutations of AML1 are common in therapy-related myelodysplasia following therapy with alkylating agents and are significantly associated with deletion or loss of chromosome arm 7q and with subsequent leukemic transformation. *Blood* 2004; **104**: 1474–1481.
5 Harada H, Harada Y, Tanaka H, Kimura A, Inaba T. Implications of somatic mutations in the AML1 gene in radiation-associated and therapy-related myelodysplastic syndrome/acute myeloid leukemia. *Blood* 2003; **101**: 673–680.
6 Zharlyganova D, Harada H, Harada Y, Shinkarev S, Zhumadilov Z, Zhunusova A *et al.* High frequency of AML1/RUNX1 point mutations in radiation-associated myelodysplastic syndrome around Semipalatinsk nuclear test site. *J Radiat Res* 2008; **49**: 549–555.
7 Kuo MC, Liang DC, Huang CF, Shih YS, Wu JH, Lin TL *et al.* RUNX1 mutations are frequent in chronic myelomonocytic leukemia and mutations at the C-terminal region might predict acute myeloid leukemia transformation. *Leukemia* 2009; **23**: 1426–1431.
8 Ernst T, Chase A, Zoi K, Waghorn K, Hidalgo-Curtis C, Score J *et al.* Transcription factor mutations in myelodysplastic/myeloproliferative neoplasms. *Haematologica* 2010; **95**: 1473–1480.
9 Matheny CJ, Speck ME, Cushing PR, Zhou Y, Corpora T, Regan M *et al.* Disease mutations in RUNX1 and RUNX2 create nonfunctional, dominant-negative, or hypomorphic alleles. *EMBO J* 2007; **26**: 1163–1175.
10 Harada Y, Harada H. Molecular pathways mediating MDS/AML with focus on AML1/RUNX1 point mutations. *J Cell Physiol* 2009; **220**: 16–20.
11 Michaud J, Wu F, Osato M, Cottles GM, Yanagida M, Asou N *et al.* In vitro analyses of known and novel RUNX1/AML1 mutations in dominant familial platelet disorder with predisposition to acute myelogenous leukemia: implications for mechanisms of pathogenesis. *Blood* 2002; **99**: 1364–1372.
12 Imai Y, Kurokawa M, Izutsu K, Hangaishi A, Takeuchi K, Maki K *et al.* Mutations of the AML1 gene in myelodysplastic syndrome and their functional implications in leukemogenesis. *Blood* 2000; **96**: 3154–3160.
13 Song WJ, Sullivan MG, Legare RD, Hutchings S, Tan X, Kufrin D *et al.* Haploinsufficiency of CBFA2 causes familial thrombocytopenia with propensity to develop acute myelogenous leukaemia. *Nat Genet* 1999; **23**: 166–175.
14 Higuchi M, O'Brien D, Kumaravelu P, Lenny N, Yeoh EJ, Downing JR. Expression of a conditional AML1-ETO oncogene bypasses embryonic lethality and establishes a murine model of human t(8;21) acute myeloid leukemia. *Cancer Cell* 2002; **1**: 63–74.
15 Motoda L, Osato M, Yamashita N, Jacob B, Chen LQ, Yanagida M *et al.* Runx1 protects hematopoietic stem/progenitor cells from oncogenic insult. *Stem Cells* 2007; **25**: 2976–2986.
16 Jacob B, Osato M, Yamashita N, Wang CQ, Taniuchi I, Littman DR *et al.* Stem cell exhaustion due to Runx1 deficiency is prevented by Evi5 activation in leukemogenesis. *Blood* 2010; **115**: 1610–1620.
17 Takahashi K, Tanabe K, Ohnuki M, Narita M, Ichisaka T, Tomoda K *et al.* Induction of pluripotent stem cells from adult human fibroblasts by defined factors. *Cell* 2007; **131**: 861–872.
18 Yu J, Vodyanik MA, Smuga-Otto K, Antosiewicz-Bourget J, Frane JL, Tian S *et al.* Induced pluripotent stem cell lines derived from human somatic cells. *Science* 2007; **318**: 1917–1920.
19 Chou ST, Byrska-Bishop M, Tober JM, Yao Y, Vandorn D, Opalinska JB *et al.* Trisomy 21-associated defects in human primitive hematopoiesis revealed through induced pluripotent stem cells. *Proc Natl Acad Sci USA* 2012; **109**: 17573–17578.
20 Ye Z, Zhan H, Mali P, Dowey S, Williams DM, Jang YY *et al.* Human-induced pluripotent stem cells from blood cells of healthy donors and patients with acquired blood disorders. *Blood* 2009; **114**: 5473–5480.
21 Park IH, Arora N, Huo H, Maherali N, Ahfeldt T, Shimamura A *et al.* Disease-specific induced pluripotent stem cells. *Cell* 2008; **134**: 877–886.
22 Hiramoto T, Ebihara Y, Mizoguchi Y, Nakamura K, Yamaguchi K, Ueno K *et al.* Wnt3a stimulates maturation of impaired neutrophils developed from severe congenital neutropenia patient-derived pluripotent stem cells. *Proc Natl Acad Sci USA* 2013; **110**: 3023–3028.
23 Maclean GA, Menne TF, Guo G, Sanchez DJ, Park IH, Daley GQ *et al.* Altered hematopoiesis in trisomy 21 as revealed through in vitro differentiation of isogenic human pluripotent cells. *Proc Natl Acad Sci USA* 2012; **109**: 17567–17572.
24 Chang CJ, Bouhassira EE. Zinc-finger nuclease-mediated correction of alpha-thalassemia in iPS cells. *Blood* 2012; **120**: 3906–3914.
25 Carette JE, Pruszak J, Varadarajan M, Blomen VA, Gokhale S, Camargo FD *et al.* Generation of iPSCs from cultured human malignant cells. *Blood* 2010; **115**: 4039–4042.

26 Kumano K, Arai S, Hosoi M, Taoka K, Takayama N, Otsu M *et al.* Generation of induced pluripotent stem cells from primary chronic myelogenous leukemia patient samples. *Blood* 2012; **119**: 6234–6242.
27 Gandre-Babbe S, Paluru P, Aribeana C, Chou ST, Bresolin S, Lu L *et al.* Patient-derived induced pluripotent stem cells recapitulate hematopoietic abnormalities of juvenile myelomonocytic leukemia. *Blood* 2013; **121**: 4925–4929.
28 Seki T, Yuasa S, Fukuda K. Generation of induced pluripotent stem cells from a small amount of human peripheral blood using a combination of activated T cells and Sendai virus. *Nat Protoc* 2012; **7**: 718–728.
29 Fukuchi Y, Shibata F, Ito M, Goto-Koshino Y, Sotomaru Y, Ito M *et al.* Comprehensive analysis of myeloid lineage conversion using mice expressing an inducible form of C/EBP alpha. *EMBO J* 2006; **25**: 3398–3410.
30 Ma F, Wang D, Hanada S, Ebihara Y, Kawasaki H, Zaike Y *et al.* Novel method for efficient production of multipotential hematopoietic progenitors from human embryonic stem cells. *Int J Hematol* 2007; **85**: 371–379.
31 Ma F, Ebihara Y, Umeda K, Sakai H, Hanada S, Zhang H *et al.* Generation of functional erythrocytes from human embryonic stem cell-derived definitive hematopoiesis. *Proc Natl Acad Sci USA* 2008; **105**: 13087–13092.
32 Takayama N, Nishikii H, Usui J, Tsukui H, Sawaguchi A, Hiroyama T *et al.* Generation of functional platelets from human embryonic stem cells in vitro via ES-sacs, VEGF-promoted structures that concentrate hematopoietic progenitors. *Blood* 2008; **111**: 5298–5306.
33 Nakajima H, Ito M, Smookler DS, Shibata F, Fukuchi Y, Morikawa Y *et al.* TIMP-3 recruits quiescent hematopoietic stem cells into active cell cycle and expands multipotent progenitor pool. *Blood* 2010; **116**: 4474–4482.
34 Seki T, Yuasa S, Oda M, Egashira T, Yae K, Kusumoto D *et al.* Generation of induced pluripotent stem cells from human terminally differentiated circulating T cells. *Cell Stem Cell* 2010; **7**: 11–14.
35 Xu MJ, Tsuji K, Ueda T, Mukouyama YS, Hara T, Yang FC *et al.* Stimulation of mouse and human primitive hematopoiesis by murine embryonic aorta-gonad-mesonephros-derived stromal cell lines. *Blood* 1998; **92**: 2032–2040.
36 Vodyanik MA, Thomson JA, Slukvin II. Leukosialin (CD43) defines hematopoietic progenitors in human embryonic stem cell differentiation cultures. *Blood* 2006; **108**: 2095–2105.
37 Choi KD, Yu J, Smuga-Otto K, Salvagiotto G, Rehrauer W, Vodyanik M *et al.* Hematopoietic and endothelial differentiation of human induced pluripotent stem cells. *Stem Cells* 2009; **27**: 559–567.
38 Dowdy CR, Xie R, Frederick D, Hussain S, Zaidi SK, Vradii D *et al.* Definitive hematopoiesis requires Runx1 C-terminal-mediated subnuclear targeting and transactivation. *Hum Mol Genet* 2010; **19**: 1048–1057.
39 Okuda T, van Deursen J, Hiebert SW, Grosveld G, Downing JR. AML1 the target of multiple chromosomal translocations in human leukemia, is essential for normal fetal liver hematopoiesis. *Cell* 1996; **84**: 321–330.
40 Wang Q, Stacy T, Binder M, Marin-Padilla M, Sharpe AH, Speck NA. Disruption of the Cbfa2 gene causes necrosis and hemorrhaging in the central nervous system and blocks definitive hematopoiesis. *Proc Natl Acad Sci USA* 1996; **93**: 3444–3449.
41 North T, Gu TL, Stacy T, Wang Q, Howard L, Binder M *et al.* Cbfa2 is required for the formation of intra-aortic hematopoietic clusters. *Development* 1999; **126**: 2563–2575.
42 North TE, de Bruijn MF, Stacy T, Talebian L, Lind E, Robin C *et al.* Runx1 expression marks long-term repopulating hematopoietic stem cells in the midgestation mouse embryo. *Immunity* 2002; **16**: 661–672.
43 Lancrin C, Sroczynska P, Stephenson C, Allen T, Kouskoff V, Lacaud G. The haemangioblast generates haematopoietic cells through a haemogenic endothelium stage. *Nature* 2009; **457**: 892–895.
44 Chen MJ, Yokomizo T, Zeigler BM, Dzierzak E, Speck NA. Runx1 is required for the endothelial to haematopoietic cell transition but not thereafter. *Nature* 2009; **457**: 887–891.
45 Ran D, Shia WJ, Lo MC, Fan JB, Knorr DA, Ferrell PI *et al.* RUNX1a enhances hematopoietic lineage commitment from human embryonic stem cells and inducible pluripotent stem cells. *Blood* 2013; **121**: 2882–2890.

Supplementary Information accompanies this paper on the Leukemia website (http://www.nature.com/leu)